

**Combustion and Propulsion Research Laboratory
Mechanical and Industrial Engineering Department
The University of Texas at El Paso
El Paso, TX 79968**

**Final Technical Report on
Department of Energy Grant DE-FG26-03NT41917**

Entitled

Investigation on the Flame Extinction Limit of Fuel Blends

**Author
Ahsan R. Choudhuri, PhD**

February 2005

Disclaimer

This report was prepared as an account of work sponsored by an agency of the United States Government. Neither the United States Government nor any agency thereof, nor any of their employees, makes any warranty, express or implied, or assumes any legal liability or responsibility for the accuracy, completeness, or usefulness of any information, apparatus, product, or process disclosed, or represents that its use would not infringe privately owned rights. Reference herein to any specific commercial product, process, or service by trade name, trademark, manufacturer, or otherwise does not necessarily constitute or imply its endorsement, recommendation, or favoring by the United States Government or any agency thereof. The views and opinions of authors expressed herein do not necessarily state or reflect those of the United States Government or any agency thereof.

Project Information

Project Title: Investigation on the Flame Extinction Limit of Fuel Blends

Grant No: DE-FG26-03NT41917

Agency: National Energy Technology Laboratory
Department of Energy

Program: Support of Advanced Fossil Resource Utilization Research by Historically Black Colleges and Universities and Other Minority Institutions

DOE Project Manager: Ben Hsieh
U.S. Department of Energy
National Energy Technology Laboratory
3610 Collins Ferry Rd.
P.O. Box 880
Morgantown, WV 26507-0880
Tel: (304) 285-4065

Amount: \$19,999

Project Period: 9/30/2003-09/29/2004

Principal Investigator: Ahsan R. Choudhuri, PhD
Assistant Professor

Contact Address: Department of Mechanical and Industrial Engineering
The University of Texas at El Paso
500 West University, Mail Stop: 0521, El Paso, Texas 79968
Tel: 915 747 6905, Fax: 915 747 5019, E-mail: ahsan@utep.edu

Students: (i) Rogelio Franco (ii) Mahesh Subramanya

Preface

This is the final technical report on DOE Grant DE-FG26-03NT41917 entitled “Investigation on the Flame Extinction Limit of Fuel Blends”. Technical work supported by this grant is described in detail in one Master of Science thesis and one PhD general exam report.

Abstract

Lean flame extinction limits of binary fuel mixtures of methane (CH₄), propane (C₃H₈), and ethane (C₂H₆) were measured using a twin-flame counter-flow burner. Experiments were conducted to generate an extinction equivalence ratio vs. global stretch rate plot and an extrapolation method was used to calculate the equivalence ratio corresponding to an experimentally unattainable zero-stretch condition. The foregoing gases were selected because they are the primary constituents of natural gas, which is the primary focus of the present study. To validate the experimental setup and methodology, the flame extinction limit of pure fuels at zero stretch conditions were also estimated and compared with published values. The lean flame extinction limits of methane ($f_{\text{ext}} = 4.6\%$) and propane ($f_{\text{ext}} = 2.25\%$) flames measured in the present study agreed with the values reported in the literature. It was observed that the flame extinction limit of fuel blends have a polynomial relation with the concentration of component fuels in the mixture. This behavior contradicts with the commonly used linear Le Chatelier's approximation. The experimentally determined polynomial relations between the flame extinction limits of fuel blends (i.e. methane-propane and methane-ethane) and methane concentration are as follows:

Methane-Propane

$$\%f_{\text{ext}} = (1.05 \times 10^{-9})f^5 - (1.3644 \times 10^{-7})f^4 + (6.40299 \times 10^{-6})f^3 - (1.2108459 \times 10^{-4})f^2 + (2.87305329 \times 10^{-3})f + 2.2483$$

Methane-Ethane

$$\%f_{\text{ext}} = (2.1 \times 10^{-9})f^5 - (3.5752 \times 10^{-7})f^4 + (2.095425 \times 10^{-5})f^3 - (5.037353 \times 10^{-4})f^2 + 6.08980409 f + 2.8923$$

Where f_{ext} is the extinction limits of methane-propane and methane-ethane fuel blends, and f is the concentration (% volume) of methane in the fuel mixture. The relations were obtained by fitting fifth order curve (polynomial regression) to experimentally measured extinction limits at different mixture conditions. To extend the study to a commercial fuel, the flame extinction limit for Birmingham natural gas (a blend of 95% methane, 5% ethane and 5% nitrogen) was experimentally determined and was found to be 3.62% fuel in the air-fuel mixture.

Executive Summary

Fuel blends are used in numerous practical combustors to achieve certain combustion performances (improved ignitability, higher flame stability, reduced pollution emissions etc). Besides many fossil fuels such as natural gas are inherently fuel blends since their compositions vary from one region of the country to another, as well as by season. Although flammability behavior and flame propagation velocity of individual fuels in air are fairly well characterized, understanding of flammability in binary and ternary fuel mixtures is rudimentary. The most commonly used assumption for estimating flammability of fuel mixtures is known as Le Chatelier's Rule. However, it is still unclear how well this simple theory will predict the flammability of blended fuels especially at the near limit. Motivated by these issues this project is aimed at understanding the combustion characteristics of fuel blends.

Flammability behavior of practical fuel blends was experimentally measured. Effects of mixture composition and flame stretch on the flammability limits of fuel blends were investigated. Based on experimental measurements, generalized empirical models were developed for the flame extinction behavior of fuel blends. It was observed that the flame extinction limit of fuel blends have a polynomial relation with the concentration of component fuels in the mixture. This behavior contradicts with the commonly used linear Le Chatelier's approximation. The outcomes of the project generate a robust and reliable understanding of the combustion behavior of fuel blends, which will certainly help the practical combustor designer to predict combustor performances more accurately.

The University of Texas, El Paso (UTEP) Combustion and Propulsion Research group which includes two faculty members and more than fifteen graduate and undergraduate minority students, were directly benefited from this project. The results of the project are partially included in one MS thesis and one PhD comprehensive exam report.

Contents

Abstract	i
Executive Summary	iii
Contents	v
List of Tables	vii
List of Figures	viii
Nomenclature	x
Chapter I	1
Introduction	1
I. Introduction.....	1
I (b). Project Goals	2
I (c). Organization of the Report.....	3
I (d). Combustion and Propulsion Research Laboratory	4
Chapter II	5
Literature Review	5
II.a. Flammability Limit vs. Flame Extinction Limit.....	5
II.b. Flame Extinction Limits of Fuel Blends.....	9
II.c. Effects of Loss Mechanism on Flame Extinction	10
II.d. Needs of Experimental Flame Extinction Data for Kinetic Model Validation	12
Chapter III	14
Experimental Setup and Methodology	14
III.a. Twin-Flame-Counter-Flow Burner.....	18
III.b. Cooling System	19
III.c. Fuel-Air Supply Train.....	19
III.d. Image Acquisition System	19
III.e. Nozzle Design	20
III.e.1. Derivation for Polynomial Profile Curve	20
III.e.2. Verifications of the Nozzle Design	23
III (f): Measurement Methodology	24
Chapter IV	26
Results and Discussion	26
IV (a): Flame Appearances	26
IV (b): Flame Extinction:.....	29
IV.b.1: Pure fuels: 100% Methane and 100% Propane.....	29
IV.b.2: Fuel Blends: Methane – Propane Blend	31
IV.b.3: Fuel Blend: Methane-Ethane Blend	36
IV.b.4: Natural Gas Composition	41
Chapter V.....	42
Conclusions and Recommendations	42
V.a. General Remarks	42
V.b. Conclusions.....	43
V.c. Recommendations and Future Research.....	44
Bibliography:.....	45
APPENDIX I: CAD Drawings.....	47
Manifold	47

Stem.....	48
Connector	49
Nozzle	50
APPENDIX II: Conversion of Equivalence Ratio to %-fuel and vice-versa.....	51
APPENDIX III: Air-fuel Stoichiometric ratio for fuel blends.....	52

List of Tables

Table 3.1	Nominal operating conditions under which experimental trials are conducted
Table 3.2	Instrument specifications
Table 3.3	Estimated measurement uncertainties
Table 4.1	Lower-flammability limits for methane and propane fuels [Source: Satoru, 1982]
Table 4.2	Lowest and highest fuel-percent in air-fuel mixture and its corresponding stretch-rates at extinction for methane-propane fuel blend
Table 4.3	Comparison of flame extinction limits obtained experimentally, value predicted by fifth-order polynomial and calculated by Le Chatelier's rule
Table 4.4	Lowest and highest fuel-percent in air-fuel mixture and its corresponding stretch-rates at extinction for methane-ethane fuel blend
Table 4.5:	Comparison of flame extinction limits obtained experimentally, value predicted by fifth-order polynomial and calculated by Le Chatelier's rule

List of Figures

- Figure 2.1 Stretching of flame front surface by propagation into a velocity gradient
- Figure 2.2 Twin-flame counterflow burner assembly for the flame extinction limit measurement
- Figure 3.1 Counter - flow twin flame burner set – up
- Figure 3.2 Burner set-up with air/fuel and nitrogen lines connected, system wound by copper coils with water flowing through it
- Figure 3.3 Burner nozzle exit with co - annular nitrogen exit
- Figure 3.4 Honeycombs
- Figure 3.5 Wire-meshes
- Figure 3.6 Burner profile
- Figure 3.7 Nozzle design with a fifth order polynomial burner curve and co-annular nitrogen exit
- Figure 3.8 Hotwire measurements of velocity and turbulence intensity at the exit of the burner
- Figure 4.1 Twin-flame images of 80% CH₄ – 20% C₃H₈ fuel blend, from formation to just before extinction at a flame-stretch $\sim 400 \text{ sec}^{-1}$
- Figure 4.2 Twin-flame images of 80% CH₄ – 20% C₃H₈ fuel blend, from formation to just before extinction at a flame-stretch $\sim 800 \text{ sec}^{-1}$
- Figure 4.3 Twin-flame images of 75% CH₄ – 25% C₃H₈ fuel blend, from formation to just before extinction at a flame-stretch $\sim 400 \text{ sec}^{-1}$
- Figure 4.4 Twin-flame images of 75% CH₄ – 25% C₃H₈ fuel blend, from formation to just before extinction at a flame-stretch $\sim 800 \text{ sec}^{-1}$
- Figure 4.5 Twin-flame images of 93% CH₄ – 7% C₂H₆ fuel blend, from formation to just before extinction at a flame-stretch $\sim 175 \text{ sec}^{-1}$
- Figure 4.6 Twin-flame images of 93% CH₄ – 7% C₂H₆ fuel blend, from formation to just before extinction at a flame-stretch $\sim 250 \text{ sec}^{-1}$
- Figure 4.7 Flame extinction limit for 100% methane fuel
- Figure 4.8 Flame extinction limit for 100% propane fuel
- Figure 4.9 Flame extinction limit for 95% methane – 5% propane fuel-blend
- Figure 4.10 Flame extinction limit for 92% methane – 8% propane fuel-blend
- Figure 4.11 Flame extinction limit for 89% methane – 11% propane fuel-blend
- Figure 4.12 Flame extinction limit for 80% methane – 20% propane fuel-blend
- Figure 4.13 Flame extinction limit for 75% methane – 25% propane fuel-blend
- Figure 4.14 Flame extinction limit for 18% methane – 82% propane fuel-blend
- Figure 4.15 Trend of flame extinction limit of methane-propane fuel-blends, experimental data in comparison with values predicted by Le Chatelier rule
- Figure 4.16 Flame extinction limit for 93% methane – 7% ethane fuel-blend
- Figure 4.17 Flame extinction limit for 90% methane – 10% ethane fuel-blend
- Figure 4.18 Flame extinction limit for 85% methane – 15% ethane fuel-blend
- Figure 4.19 Flame extinction limit for 81% methane – 19% ethane fuel-blend
- Figure 4.20 Flame extinction limit for 20% methane – 80% ethane fuel-blend

- Figure 4.21 Trend of flame extinction limit of methane-ethane fuel-blends, experimental data in comparison with values predicted by Le Chatelier rule
- Figure 4.22 Flame extinction limit for Birmingham fuel composition of 90% CH₄, 5% C₂H₆ and 5% N₂

Nomenclature

$\%f_{ext}$	= percent-fuel in air-fuel mixture at extinction
$\%f$	= percent-fuel in air-fuel mixture
x	= methane composition in fuel blend
$r(l)$	= radius, as a function of length
l	= length from the inlet diameter
L	= flame extinction limit for a fuel blend, calculated using Le Chatelier's rule
L_i	= flame extinction limit of i^{th} fuel in the fuel blend
x_i	= percent-composition of i^{th} fuel in fuel blend
k	= stretch-rate (sec^{-1})

Chapter I

Introduction

I. Introduction

The study of combustion characteristics of gaseous fuel blends is essential because of its importance in numerous practical applications. For instance, natural gas compositions significantly affect the emission and operational performances of natural gas turbine combustors. Although natural gas consists primarily of methane, truly it is a fuel blend of methane, ethane, propane, small amount of higher hydrocarbons and inert species. Compositions of the mixture typically vary from one region of the country to another, as well as by season. These variances induce important shifts in combustor flame behavior through kinetics and mixing effects. Recent investigations have shown that the fuel composition effects were specially pronounced at the lean burn condition, because of stringent requirements of active combustion control [El - Sherif, 1998].

Another development using fuel blends is as a mixture of hydrogen and methane called Hythane. This is particularly attractive for lean burn LNO_x gas turbine combustor and PFI internal combustion engines. The flammability limit of hydrocarbon/air mixture can be extended by adding a small amount of hydrogen, which allows LNO_x combustors to operate at highly lean conditions and an internal combustion engine to operate at near stoichiometric air/fuel ratio during cold start processes. Preliminary information presented at the 10th World Hydrogen Energy Conference indicates that a test car exhaust using 30% hydrogen and 70% methane contained 80% less nitrogen oxides than EPA standards for 2003. Also, recent investigations have suggested that if the intake air could be fumigated with hydrogen, it may be possible to extend the dilution tolerance of the

engine such that it can operate closer to stoichiometric or even fuel lean during the cold start process. Addition of gaseous fuel additives (addition of carbon monoxide, ammonia, cyanuric acid in the exhaust) to the combustion processes is also considered as one of the most effective methods (selective non-catalytic reduction) for reducing not only NO, but also NO₂ and N₂O. Similar improvements of combustion characteristics for hydrogen and hydrocarbon fuels have also been observed with the addition of silane (SiH₄) [Golovitchev et al., 1999].

Despite a lot of practical importance, little information is available regarding the combustion behavior of the mixtures of multiple fuels and oxidizers. Although it may be expected that the combustion characteristics of fuel blends will fall between those of the primary fuels, some recent investigations have clearly demonstrated that blended fuels can have radically different characteristics from those of the original fuels [Bui-Pham, 1995; Choudhuri, 2000; El-Sherif, 2000]. However, a comprehensive study to investigate the combustion behavior of fuel blends has yet to be done. Motivated by these issues, this study is aimed at understanding the flammability characteristics of fuel blends.

I (b). Project Goals

The overall objective of this project is to understand the flame extinction behavior of fuel blends. However, the current study concentrates on generating flammability (flame extinction limit) maps of different compositions of methane-propane and methane ethane fuel blends with varying stoichiometry. This particular fuel combinations were selected because they are the primary constituents of the natural gas and the extinction

behavior of natural gas is the primary focus of the present study. The influence of mixture composition and flame stretch rate on flame extinction behavior of hydrocarbon fuel blends was studied. Since most of the fuel blends have peculiar behavior at the limit, the present study measured only the lean extinction of blended fuel flames. Based on experimental measurements, a generalized empirical model was sought for the flame extinction behavior of methane-propane and methane-ethane fuel blends. Validity of the currently practiced flame extinction limit rule (Le Chatelier approximation) for fuel blends was also investigated.

I (c). Organization of the Report

The approach used to fulfill the primary objective, and results obtained are discussed in five chapters. In *Chapter 1*, followed by the Introduction are the project motivation and objectives, organization of the report and a brief description of the laboratory. *Chapter 2* contains the background information and literature review which are essential to understand the objectives and outcomes of the project. The chapter explains various aspects of flame extinction behavior of flames. The discussions are provided in the context of blended fuel combustion. *Chapter 3* explains the experimental setup and the methodology used in the research. It contains figures and photographs of the experimental setup and tables of specifications of the different apparatuses used. The results and related discussions are presented in *Chapter 5*. *Chapter 6* concludes the report with a concluding discussion, specific conclusions and recommended future work.

I (d). Combustion and Propulsion Research Laboratory

The Combustion and Propulsion Research Laboratory is located in the Mechanical and Industrial Engineering Department. The laboratory has a 4880 sq-ft physical space and located in the main campus engineering complex. The laboratory contains state of the art facilities and software to conduct research on fundamental and applied combustion. Current instrumentation for mixing dynamics and combustion research includes a laser Doppler velocimeter, a microparticle image velocimeter, a LIF/PLIF/Raman Spectroscopy system, high speed and infrared imaging system, and various emission gas analyzers (non dispersive infrared and chemiluminisence). The spectroscopic system uses a pulsed tunable Laser system (Nd: YAG pumped Optical Parametric Oscillator with Frequency Doubler Option) which has a tunability range from 190 nm to 2000 nm as a light source. The detection system includes an intensified camera, a monochromator/imaging spectrograph, a nanosecond gate pulse generator/boxcar integrator and a camera controller and image acquisition hardwares.

For computational analysis, a number of workstations are available with CFD, Chemical Kinetics and Heat Transfer software (STAR-CD, CFD ACE+, Sandia PREMIX, CHEMKIN, LSENS, and Coolit). The computer facilities of CPRL include several Linux workstations and programming environments. The laboratory also shares an IBM p690 and a HP Itanium cluster with the computational mechanics laboratory. The IBM p690 is an eight way shared memory machine with each node consisting of a 1.1 GHz processor and a total of 16Gb of core memory. The HP Itanium cluster is four way distributed memory machine.

Chapter II

Literature Review

Despite numerous past research efforts, there are still uncertainties and lack of information in understanding the mechanism of flammability limits especially in the near extinction region. Effects of various factors such as flame stretch, chemical kinetics, and heat losses make it exceedingly complicated to determine flammability limits accurately. A number of empirical and semi-empirical theories and relations have already been proposed for estimating flammability limits. Different theories and ideas have been advanced to explain the flammability phenomena and its relation with above mentioned factors and test protocols. A comprehensive review of these theories can be found in Lewis et al. [1987] and Hertzberg [1976].

II.a. Flammability Limit vs. Flame Extinction Limit

It is important to note that the implication of the term ‘flammability limit’ is different from the safety community to the basic combustion research community. Safety studies are primarily concerned with experimentally determining the limiting concentrations beyond which combustion can be assured not to occur. Hence, the experimental evaluation of such limits is highly apparatus and test protocol dependent. For instance, the determination of lean flammability based on the current American Society of Testing and Materials (ASTM) standard depends on the ignition and brief propagation of a flame in 5 liter and 20 liter vessels filled with the well-mixed, quiescent, flammable gas mixture. This standard attempts to define a clear distinction between the mixture that creates a non-propagating flicker and a flame that has enough horizontal

propagation to be hazardous. Clearly, determination of flammability using this protocol depends on the ignition source, energy and criteria for determining when ignition has occurred. Hence, this type of flammability limit is often termed as ‘ignition limit’.

Basic combustion researchers prefer to define the flammability limit as a state of fuel and oxidizer mixture at which steady propagation of a one-dimensional premixed flame fails to be possible [Spalding, 1957]. As it was mentioned earlier, fuel type, mixture properties and mass diffusion of the deficient reactants are all factors in defining the limiting compositions. Generally, the theoretical determination of a limit is tied to a specific configuration, a chemical kinetics mode, diffusive and radiative transport models, and numerical solution methods. From the theoretical perspective, limits arise because mechanisms such as chain-terminating reactions, radiative heat loss, and preferential diffusion eventually dominate the energy release mechanism and cause the extinction of the flame at the limit. This type of flammability definition is termed as ‘flame extinction limit’.

Although, there has been some recent progress towards connecting these two approaches to flammability, a comprehensive study addressing this issue has yet to be published [Pfahl et al., 2000]. Typically, standard flame tube and constant volume combustion chamber are used to determine the ignition limit. For instance, Coward and Jones [1952] proposed measurement of the ignition limit using a standardized tube (180 cm long and 5 cm diameter) and termed as standard flammability limit. According to this test protocol, a mixture of fuel and oxidizer are flammable, (ignitable) if they sustain flame propagation throughout the tube. Other test protocols are also developed to account for the effects of various parameters (tube size, ignition energy etc.) on flammability

measurements. The measurement done by Coward and Jones [1952] showed that flammability limits (ignition limit) are different for flame propagation in the upward, downward and horizontal directions of propagation.

The most widely accepted technique for determining the flame extinction limit utilizes a twin flame counterflow arrangement proposed by Law et al. [1990]. This technique uses a planar, twin-flame-counterflow nozzle system to determine the stretch rate at which flames are extinguished. By repeating the experiment at diminishing fuel/air ratios, it is possible to plot the equivalence ratio versus the extinction stretch rate, and to extrapolate the results to identify the equivalence ratio corresponding to an experimentally unattainable zero-stretch condition. Flame stretch is an alteration

phenomenon in the flame front shape, caused due to its propagation into a velocity gradient field. The concept of flame stretch as explained by Karlovitz [Hertzberg, 1976] with reference to figure 2.1 is, quote “At point 1 the combustion wave enters the segment 1-2 with the small velocity component $U_1 \cos\phi_1$, parallel to the wave surface; at point 2 it leaves with the larger velocity component $U_2 \cos\phi_2$. Thus new flame surface is produced

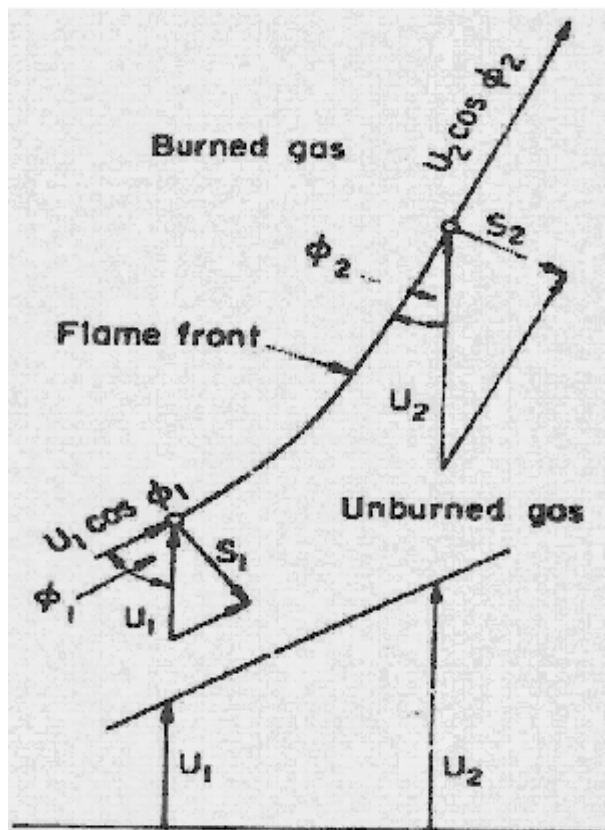


Figure 2.1: Stretching of flame front surface by propagation into a velocity gradient

continually as the flame transverses the velocity gradient. As a consequence of this ‘stretching’ of the flame surface, the amount of heat flowing from the reaction zone of the flame into the unburned gas is distributed over increasing volumes of gas, which means that the burning velocity must decrease.” In a twin-flame counterflow burner assembly, the global stretch rate is defined by the ratio of the air-fuel exit velocity to the distance of the flame front to the burner. Figure 2.2 shows a generalized schematic diagram of the counterflow burner setup assembly.

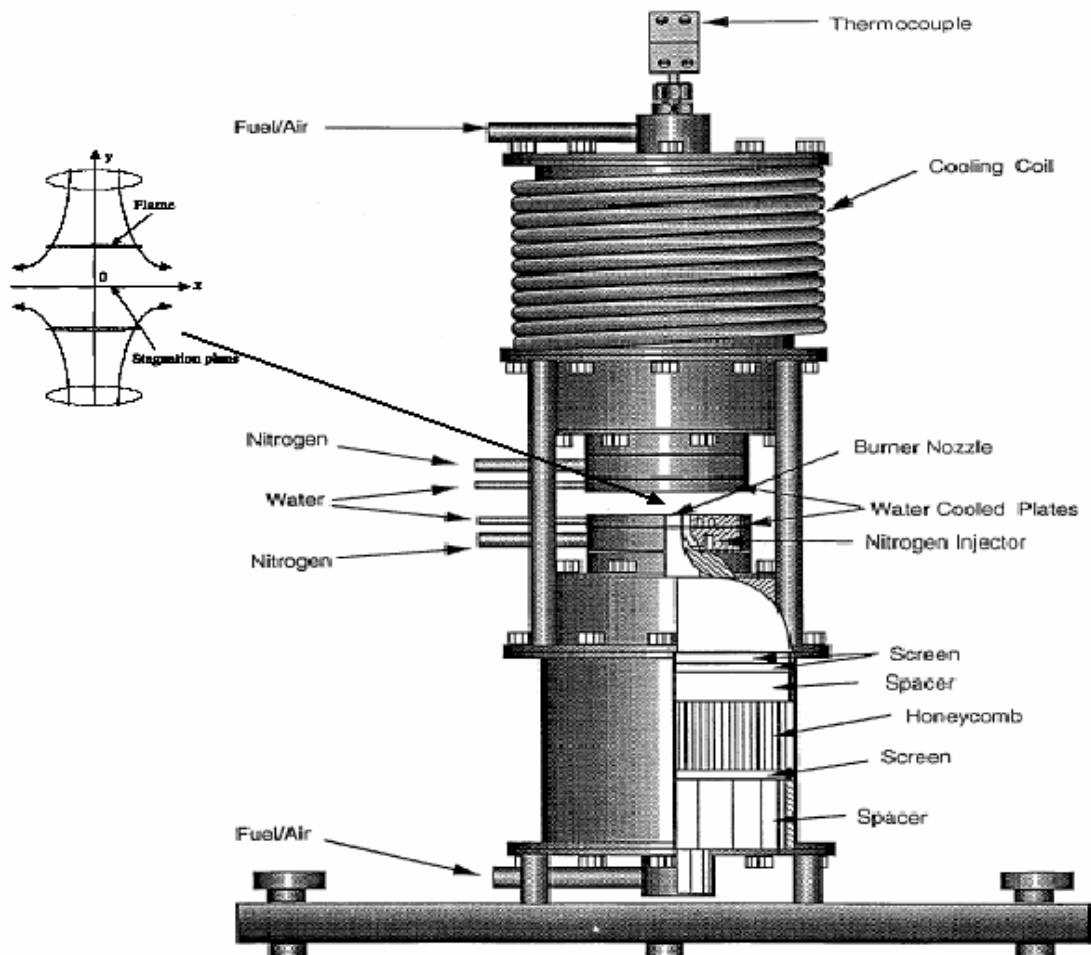


Figure 2.2: Twin-flame counterflow burner assembly for the flame extinction limit measurement

Unlike the ignition method, this technique entirely avoids issues associated with the ignition system. It also minimizes heat loss and wall effects and it is amenable to computational analysis. The current research focused its effort to measure flame extinction limit in order to understand the fundamental flame dynamics of fuel blends.

II.b. Flame Extinction Limits of Fuel Blends

Understanding flame propagation or flammability of binary and ternary fuel (usually termed as blended fuel) mixtures is rudimentary. The most common assumption is known as Le Chatelier's Rule¹. According to this rule flammability in binary and ternary fuel mixtures is that the limiting mole fractions X_i of each species ' i '. However, it is still unclear how well this simple theory will predict the flammability limit of multiple fuel mixtures especially at the limit. Bui-Pham et al. [1995] have made a detailed comparison of limits determined experimentally with spark and chemical igniters to predictions based on adiabatic, steady, laminar flame computations for the flammability limit of CH₃OH/CO/ diluent mixtures in O₂. Two simple ideas were examined: (1) a limit flame speed of 5 cm/s; and (2) equality of primary chain termination rates and radical production rates. Although the predicted trends for critical oxygen concentration with pressure and diluent type were qualitatively correct, the quantitative values were not. Furthermore, as Bui-Pham et al. [1995] reported, intrinsic flammability limits and ignitability appears to be two distinct phenomena. The most striking result was the existence of mixtures that could be ignited and burned completely

¹ $\sum_{fuels} \frac{X_i}{X_{i,LFL}} = 1$ at mixture Lower Flammability Limit. Where $X_{i,LFL}$ is the limit concentration for a single fuel species ' i ' in the oxidizer-diluent mixture of interest.

although they were apparently outside the theoretically determined flammability limit. Clearly such results indicate that the prediction of flammability of mixed fuels is an active research area and substantial gaps remains between present theoretical understanding and industrial practice. Although experimental flammability limits in the individual fuels in air are fairly well characterize, very little data exists regarding the flammability limits of various fuel oxidizer combinations.

II.c. Effects of Loss Mechanism on Flame Extinction

Despite the differences in measurement methodology, fundamentally the flame extinction limit of a fuel mixture hinges on two basic phenomenon of combustion; (i) flame velocity and (ii) loss mechanisms. A study with moist carbon monoxide has shown that the flame speed is raised considerably by an addition of a very small amount of hydrogen or hydrogen-containing fuels. Pitts [1989]. Yu et al. [1986] have also investigated the addition of hydrogen in methane. They have shown that their measured values of laminar flame speed vary quasi-linearly with a specially defined parameter, R_H indicates the contribution of hydrogen in the composite fuel. However, R_H varies nonlinearly with fuel mole fraction, and thus the laminar flame speed has a nonlinear relation with hydrogen content in the mixture. Furthermore, two crucial assumptions, i.e., complete oxidation of hydrogen and non-existence of competitive reactions, made in deriving R_H make this concept less attractive for use in diffusionally-controlled flames. Choudhuri and Gollahalli [2004, 2003a, 2003b, 2000a, 2000b] have presented a technique to compute the maximum laminar flame speed of mixed fuel based on the diffusion theory. Their calculation utilizes the theory proposed by Tanford and Pease [1947] which assumed that the rate of diffusion of active radicals into the unburned gas

determines the magnitude of the flame velocity. They have also demonstrated that the concentrations of H, OH, CH radicals are important factors in determining the laminar flame velocity.

Most of the previous studies have shown that flame velocity at the extinction limit is non-zero. For example, computations done by Lakshmisha et al. [1990] and Giovangigli and Smokee [1992] have clearly demonstrated that without losses there is no chemical extinction limit exists for planar unstretched flames. Extinction limits arise when heat loss and termination of chain branching reactions suppress energy releasing chemical reactions. The idea of heat losses creating a limiting condition was first advanced by Spalding [1957]. Law and Egolfopoulos [1990] have shown that turning points in one-dimensional steady laminar flame computations with a simplified radiative loss model correlated reasonably well with known experimental limits for lean methane-air and rich-hydrogen-air mixtures.

More recent studies [Sung et al., 1996] have shown that the situation is substantially more complex when the combined effects of strain and radiation are considered, particularly for mixtures with Lewis numbers less than unity. Although in the last ten years several investigations have been done at 1g and microgravity to understand the loss mechanisms, it is still unclear how multiple fuel and oxidizer combinations affect those mechanisms. For example, typically increasing dilution increases the heat losses, which eventually leads to the extinction limit.

When hydrogen is mixed with methane and burned in air, the difference in flame speeds causes methane to act as a diluent for some stoichiometries. Hence, the extinction limit of the mixture decreases. However, it is interesting to note that after a certain

concentration, further increases in methane in hydrogen-methane mixtures cause the increase of radiation reabsorption effect which actually increases the flammability of the mixture. Earlier, Choudhuri and Gollahalli [2000a] observed that in hydrogen-methane fuel mixtures when methane concentration exceeded 20% of the mixture the effective flame radiation decreased due to radiation reabsorption phenomena. An increase in methane concentration in mixture (>30%) causes a rapid increase of the volumetric concentration of solid soot particles which results in self-absorption of radiation, leading to a decrease in the radiant energy losses to the surroundings [Choudhuri and Gollahalli, 2000b]. They have also observed similar effects in methane-propane mixtures.

Recently, through microgravity combustion experiments, Abbud-Madrid and Ronny [1993] have shown that the radiation re-absorption effect indeed increases the flammability limit of the mixture. By using particle seeded gas mixtures they have demonstrated that for a 5.25% methane-air mixture, as the particle loading was increased, the laminar flame speed decreased at first then increased to a value near or above that of particle free mixtures. So, understanding the loss mechanism in pure fuel is not enough to predict the loss phenomena in multiple fuel-oxidizer mixtures. Since, most of the practical fuels are indeed mixtures of multiple reactive components, further study is justified to properly understand how loss mechanisms behave at multiple fuels-oxidizer conditions. From this perspective the proposed study enhance the understanding of fundamental combustion behaviors of practical fuels.

II.d. Needs of Experimental Flame Extinction Data for Kinetic Model Validation

Recently, several investigators have investigated the flammability behavior of mixed fuels through detailed chemical kinetic computations. El-Sherif [2000]

investigated the effects of adding hydrogen and carbon monoxide in a methane-air flame to control nitrogen oxide and carbon monoxide emission. The mixed fuel ($\text{H}_2\text{-CO-CH}_4$) flames were simulated by a one-dimensional model incorporating detailed representation of transport fluxes and chemical kinetics which involves $\text{CH}_4/\text{H}_2/\text{CO}/\text{NO}_x$ chemistry (59 reactions, 25 chemical species). His investigation especially pointed out the unavailability of lean flammability data for multiple fuel mixture for analyzing the validity of computations. In an effort to lower the cold start hydrocarbon emission, Sung et al. [2001] investigated the characteristics of n-Butane and iso-Butane flames mixed with reformer gas ($\text{H}_2\text{-CO}_2\text{-N}_2$). Using Sandia's PREMIX and CHEMKIN chemical kinetics computer codes they computed the lean flammability limit and the flame propagation velocity of the mixed fuel. Golovitchev and Bruno [1999] have also developed kinetic models for hydrogen-silane mixtures. Once again lack of experimental data restricted them to evaluating the accuracy of their prediction. To date, in practically all comparisons for lean premixed hydrocarbon-air flames, the computational models predict higher flame velocity and leaner flammability limits than the experimental observations. In this context more experimental data of flame extinction characteristics of practical blended fuels are absolutely essential to develop reliable kinetics models.

Chapter III

Experimental Setup and Methodology

The experimental set-up primarily consists of a counter-flow burner, a water-cooling system, fuel-air supply train and image acquisition systems. The nozzle, in particular, was designed to generate a uniform flow velocity at the burner exit, and is discussed in detail in Section III (e). Section III (f) presents the experimental methodology, test matrix and nominal operating conditions (Table 3.1), under which experimental trials are conducted. The instrumentation specifications are shown in Table 3.2. Also, photographs of experimental setup and instrumentation are presented in Figures 3.1, 3.2 and 3.3. The detailed CAD files of the burner system are provided in Appendix I. The estimated measurement uncertainties were given in Table 3.3.

Fuel Blends	100% CH ₄ , 100% C ₃ H ₈ , 95% CH ₄ - 5% C ₃ H ₈ , 92% CH ₄ - 8% C ₃ H ₈ , 89% CH ₄ - 11% C ₃ H ₈ , 86% CH ₄ - 14% C ₃ H ₈ , 80% CH ₄ - 20% C ₃ H ₈ , 75% CH ₄ - 25% C ₃ H ₈ , 18% CH ₄ - 82% C ₃ H ₈ , 93% CH ₄ - 7% C ₂ H ₆ , 90% CH ₄ - 10% C ₂ H ₆ , 85% CH ₄ - 15% C ₂ H ₆ , 81% CH ₄ - 19% C ₂ H ₆ , 20% CH ₄ - 80% C ₂ H ₆
Ambient Temperature	300 K
Ambient Pressure	101.25 kPa

Table 3.1: Nominal operating conditions under which experimental trials are conducted

Instrument	Model/Manufacturer	Specifications		
Image Acquisition	JAI CV-S3200		PAL	NTSC
		Scanning System	625 lines	525 lines
			25 frames/sec	30 frames/sec
		CCD Sensor	Color 1/2" and 1/3" IT Exview HAD CCD	
		Sensing Area	6.6 (h) x 4.8 (v) mm	
		Picture elements eff.	752 (h) x 528 (v)	768 (h) x 494 (v)
		Cell size: 1/2"	8.6 x 8.3 μ m	8.4 x 9.8 μ m
		Resolution (horizontal)	> 450 TV lines	
		S/N ratio	> 50 dB (AGC off, Gamma 1.0)	
		Video Output	1.0 Vpp, 75 Ohm, VBS and Y/C	
		Power	12V DC 3W	
		Dimensions	45 x 55 x 110.2mm (HxWxD)	
Weight	350 g			
Image Recorder	Panasonic WJ-HD100	Power consumption	24W	
		Operating Temperature	+5 - +45 °C	
		Dimensions (WxHxD)	420 x 44 x 350mm	
		Weight	5.2 kg	
Image Acquisition Computer	Dell P4	Processor Speed	2.4 GHz	
		RAM	512 MB	
Transverse Mechanism	Velmex	Program Storage (memory type)	5 (RAM/FLASH)	
		Interface	RS-232	
		Step/Rev	400	
		Speed Range (steps/sec)	1 to 6000	
		Default Baud Rate	9600	
		Maximum Baud Rate	38,400	
		Manual Jog Inputs (Front Panel)	Yes	
Program language	ASCII Characters			
Flow-meters	FMA 5600	Accuracy	\pm 1.5% of full scale	
		Repeatability	0.5% of full scale	
		Temperature Coefficient	0.15% of full scale/°C	
		Pressure Coefficient	0.01% of full scale/psi (0.07 bar)	
		Response Time	300ms time constant; approximately 1 sec to within \pm 2% of set flow rate for 25% to 100% of full scale flow	
		Gas Pressure	500 psig (34.5 bars) maximum 20 psig (1.4 bars) optimum pressure	
		Gas and Ambient Temperature	32 °F to 122 °F (0 °C to 50 °C)	
		Relative Gas Humidity	up to 70%	
		Leak Integrity	1 x 10 ⁻⁷ sccs He max to the outside environment	
Transducer Input Power	+ 12 VDC, 1100 mA			
Cooling water circulation pump	Teel 9HK96	Volts	115/230	
		Frequency	60 Hz	
		Amperes	12.4/6.2	
		Power	1 HP	

Table 3.2: Instrument specifications

Measurements	% of Mean Value
Flame Extinction Limit:	
100% CH ₄	1.4%
100% C ₃ H ₈	1.6%
95% CH ₄ - 5% C ₃ H ₈	1.3%
92% CH ₄ - 8% C ₃ H ₈	1.4%
89% CH ₄ - 11% C ₃ H ₈	1.5%
86% CH ₄ - 14% C ₃ H ₈	1.2%
80% CH ₄ - 20% C ₃ H ₈	1.3%
75% CH ₄ - 25% C ₃ H ₈	1.4%
18% CH ₄ - 82% C ₃ H ₈	1.4%
93% CH ₄ - 7% C ₂ H ₆	1.3%
90% CH ₄ - 10% C ₂ H ₆	1.7%
85% CH ₄ - 15% C ₂ H ₆	1.2%
81% CH ₄ - 19% C ₂ H ₆	1.5%
20% CH ₄ - 80% C ₂ H ₆	1.1%

Table 3.3: Estimated measurement uncertainties

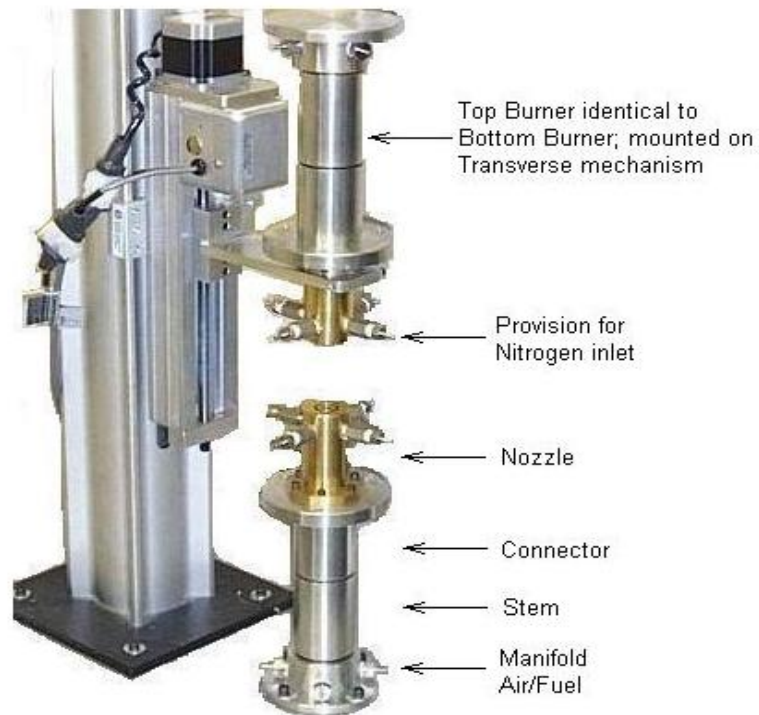


Figure 3.1: Counter - flow twin flame burner set - up

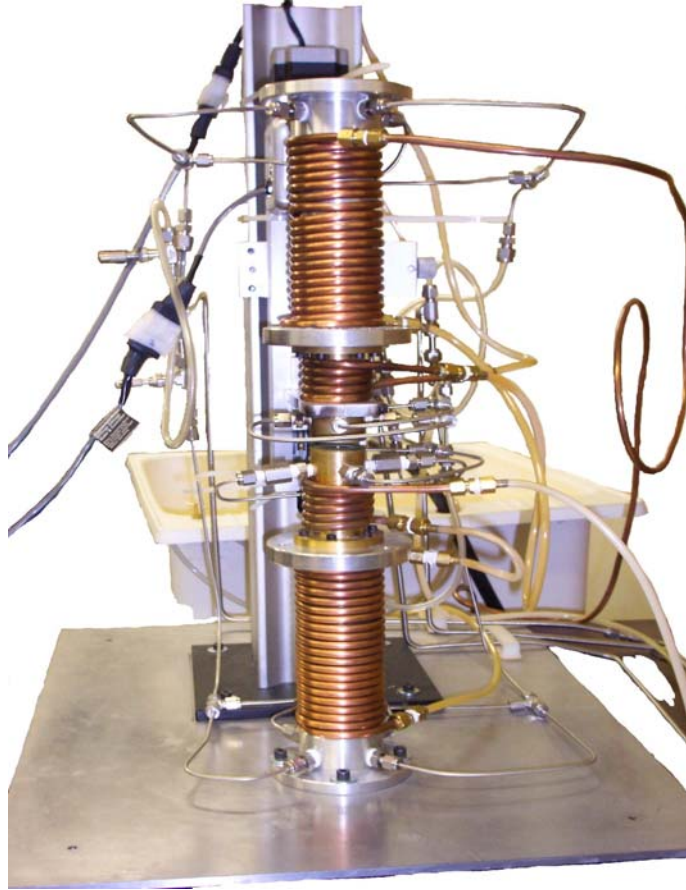


Figure 3.2: Burner set-up with air/fuel and nitrogen lines connected, system wound by copper coils with water flowing through it

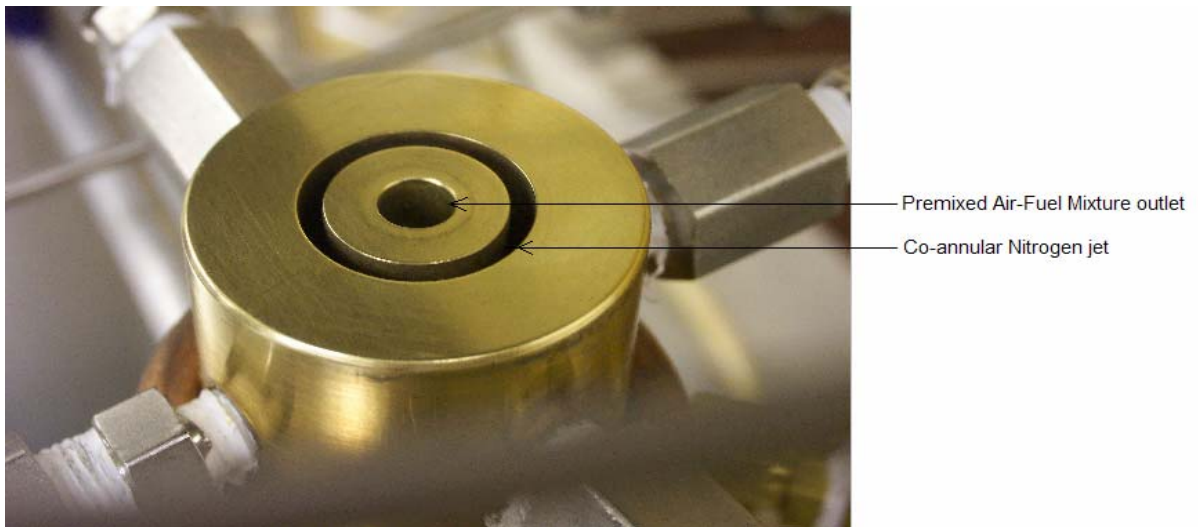


Figure 3.3: Burner nozzle exit with co - annular nitrogen exit

III.a. Twin-Flame-Counter-Flow Burner

The counter flow burner system comprises of two identical burners facing each other. The top burner is mounted on a computer controlled precision traverse system (precision lead screw, stepper motor, motor controller, digital position sensor and necessary software) which allow to change the position of the top burner to create a predetermined flame stretch. The traverse system provides a positional accuracy of 0.00254mm. Of the four distinctive parts in the burner; the manifold, stem, connector and nozzle, first three were fabricated with aluminum alloy, selected for its lightweight and good thermo-mechanical properties. The stem and connector in burner



Figure 3.4: Honeycombs



Figure 3.5: Wire-meshes

set-up allows air-fuel mixture flow to stabilize before entering the burner exit profile. Honeycombs (Figure 3.4) and wire meshes (Figure 3.5) are used inside the stem to condition the incoming flow. The nozzle was fabricated using brass alloy to ensure minimal deformation of burner profile due to high temperatures formed during combustion processes. The nozzle is surrounded by an internally machined conannular passage. The internal nozzle profile satisfies a fifth-order polynomial equation whose coefficients were calculated using flow boundary equations. The fifth order profile of the nozzle ensures a uniform velocity profile at the exit, which is necessary to create high quality twin flames amenable to stretch extinction. Nozzle design and exit velocity profiles of the top and bottom burners are presented later in section III (e).

III.b. Cooling System

Nitrogen was passed through a concentric annulus around the nozzle to create an inert environment around the flame and to trim the edges of the one-dimensional twin-flame. The nitrogen also cooled the nozzle and to maintain the burner tip temperature within an acceptable limit. A water cooling system comprises with copper cooling coils, a water sump and a centrifugal pump was also used. Cold water (25 °C) was also continuously pumped through the cooling coils wrapped around the burner to control the temperature of the entire system. A typical experimental trial required to estimate extinction limit of flames was about one minutes and the temperature of the system rose around 10-14 °C during each trial. Adequate time intervals between trials between each trial were provided to ensure acceptable temperature of the burner.

III.c. Fuel-Air Supply Train

The fuel gas supply train consisted of methane, propane, nitrogen and air cylinders, two stage pressure regulators, digital flow meters, inline filters and stainless steel tubings and connectors. Methane, ethane, propane and air were metered, and fed through individual lines into the manifold. Digital mass flow controllers and precision needle valves were used to meter and control the gas flow rates.

III.d. Image Acquisition System

A magnified real-time image of the flame was displayed and recorded using a high resolution digital camera and DVD recorder system. These flame images were used to fine tune the alignment of the burners. An enlarged flame image facilitated better judgment at flame extinction. In addition, the image acquisition system was used to

acquire high resolution color pictures at different fuel mixtures and equivalence ratios for the analysis of flame appearances.

III.e. Nozzle Design

As mentioned earlier, a fifth-order polynomial equation was used to generate the inner profile of the nozzle. The polynomial equation defines radius at a point as a function of its height. Differentiating the equation and using boundary conditions compute coefficients for this polynomial equation. Detailed computation of the polynomial curve is discussed below. Figure 3.6 presents the burner profile and 3.7 presents the SolidWorks drawing of the nozzle design in the burner.

III.e.1. Derivation for Polynomial Profile Curve

Shown below were the general polynomial equations with letters $a - f$ being the coefficients to be solved; r is the radius and l is the length of the curve.

- $r = al^5 + bl^4 + cl^3 + dl^2 + el + f$
- $r = bl^4 + cl^3 + dl^2 + el + f$
- $r = cl^3 + dl^2 + el + f$

Beginning the derivation of the 5th order polynomial equation

- Position Equation:

$$r = al^5 + bl^4 + cl^3 + dl^2 + el + f$$

- First Derivative: Slope

$$\frac{dr}{dx} = 5al^4 + 4bl^3 + 3cl^2 + 2dl + e$$

- Second Derivative: Inflection Point

$$\frac{d^2 r}{dx^2} = 20al^3 + 12bl^2 + 6cl + 2d$$

Boundary Conditions

$$\begin{array}{llll} x = 0 & r = 0.5 \text{ inches} & \partial r / \partial x = 0 & \partial^2 r / \partial x^2 = 0 \\ x = \ell & r = 0.125 \text{ inch} & \partial r / \partial x = 0 & \partial^2 r / \partial x^2 = 0 \end{array}$$

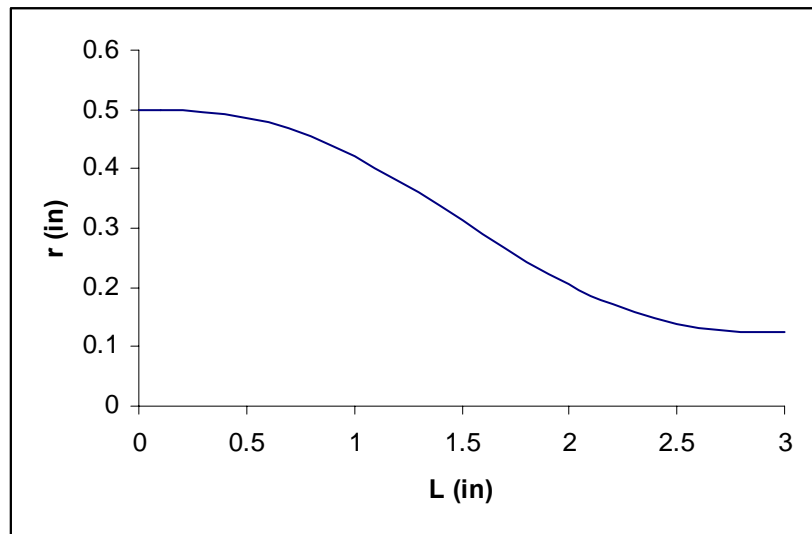


Figure 3.6: Burner profile

Applying Boundary Conditions

$$\mathbf{BC \#1: @ } x = 0 \quad r = 0.5 \text{ inches} \quad \partial r / \partial x = 0 \quad \partial^2 r / \partial x^2 = 0$$

$$\begin{aligned} r(0) &= al^5 + bl^4 + cl^3 + dl^2 + el + f \\ 0.5 &= f \end{aligned}$$

$$\begin{aligned} \frac{dr}{dx} &= 5al^4 + 4bl^3 + 3cl^2 + 2dl + e \\ 0 &= e \end{aligned}$$

$$\begin{aligned} \frac{d^2 r}{dx^2} &= 20al^3 + 12bl^2 + 6cl + 2d \\ 0 &= d \end{aligned}$$

$$\text{BC \# 2: } x = \ell \quad r = 0.125\text{inch} \quad \partial r / \partial x = 0 \quad \partial^2 r / \partial x^2 = 0$$

$$r(\ell) = a\ell^5 + b\ell^4 + c\ell^3 + d\ell^2 + e\ell + f$$

$$0.125 = a\ell^5 + b\ell^4 + c\ell^3 + 0.5$$

$$-0.375 = a\ell^5 + b\ell^4 + c\ell^3$$

$$\frac{dr}{dx} = 5a\ell^4 + 4b\ell^3 + 3c\ell^2 + 2d\ell + e$$

$$0 = 5a\ell^4 + 4b\ell^3 + 3c\ell^2$$

$$\frac{d^2r}{dx^2} = 20a\ell^3 + 12b\ell^2 + 6c\ell + 2d$$

$$0 = 20a\ell^3 + 12b\ell^2 + 6c\ell$$

Simultaneous equations, three equations, three unknowns with $\ell = 4$ inches:

$$a(4)^5 + b(4)^4 + c(4)^3 = -0.375$$

$$5a(4)^4 + 4b(4)^3 + 3c(4)^2 = 0$$

$$20a(4)^3 + 12b(4)^2 + 6c(4) = 0$$

Coefficients after solving the simultaneous equations were:

$$a = -0.00925925$$

$$b = 0.0694444$$

$$c = -0.138888$$

Substituting coefficients into the position equation yields:

$$r(\ell) = -0.00925925\ell^5 + 0.0694444\ell^4 - 0.138888\ell^3 + 0.5$$

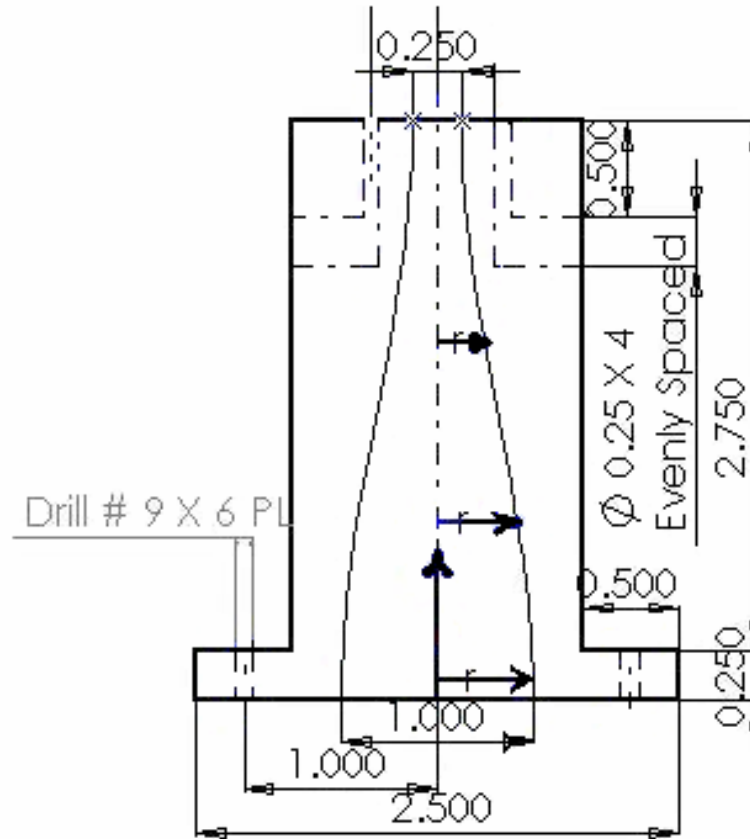


Figure 3.7: Nozzle design with a fifth order polynomial burner curve and co-annular nitrogen exit

III.e.2. Verifications of the Nozzle Design

The nozzle was fabricated using CNC milling and lathe machines. The measured velocity profiles at the nozzle exit for both burners are shown in Figure 3.8. The measured exit velocities confirm the top hat velocity profile at the burner exit. In addition less than 1% turbulent fluctuations in most cases showed the well conditioned flow through wire meshes and flow straightners.

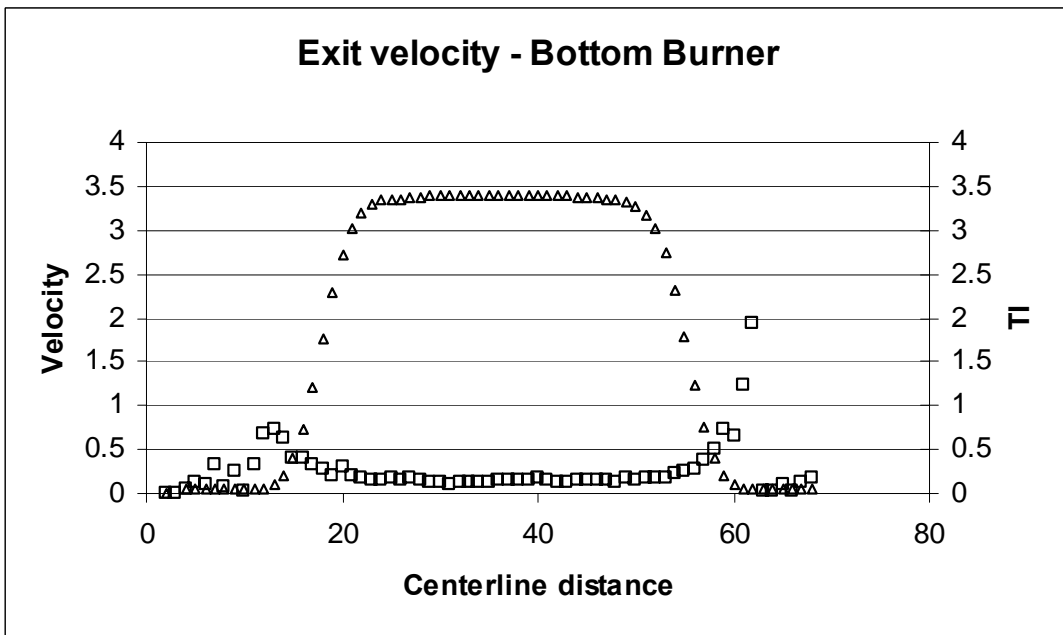
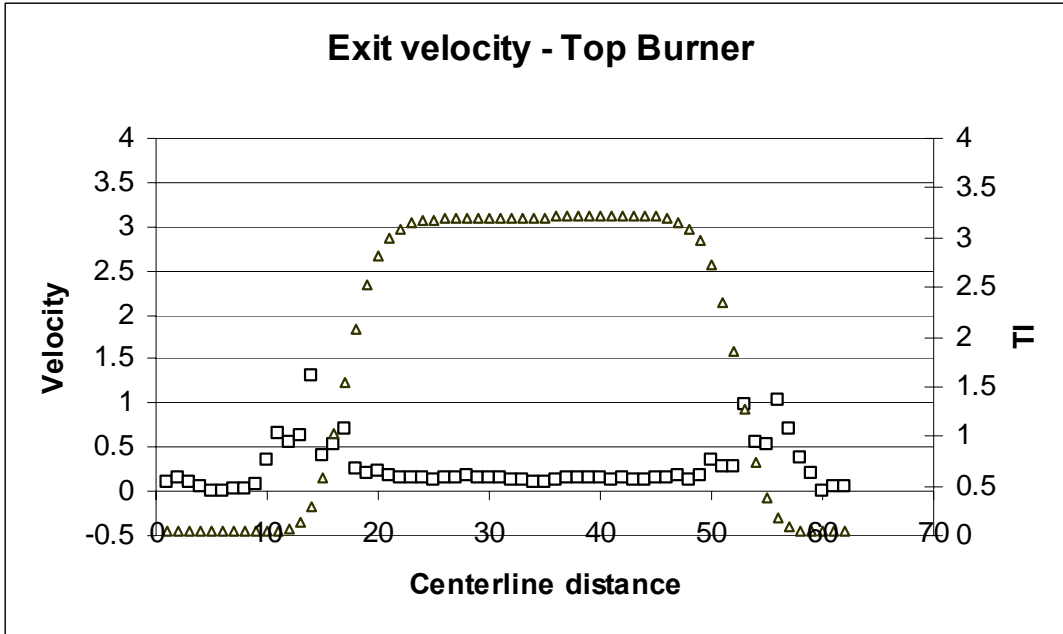


Figure 3.8: Hotwire measurements of velocity and turbulence intensity at the exit of the burner

III (f): Measurement Methodology

Flame extinction limits of pure fuels (methane and propane) were initially measured to validate the experimental apparatus and procedure. Experiments were

conducted to determine the stretch-rates at flame-extinction of lean air-fuel mixtures. Twin-flames with air-fuel mixture ranging from a maximum equivalence ratio of 0.9 through the lowest experimentally achievable equivalence ratio (all results presented and discussed in terms of percent-fuel in air-fuel mixture) were studied. An extrapolation of the percent-fuel in air-fuel mixture to zero-stretch yielded the flame extinction limit of the fuel.

The flame extinction limits of methane with different volumetric percentages propane ethane in mixtures were then determined. For a particular volumetric-percentage of methane in the methane-propane or methane-ethane fuel-blend mixture, stretch-rates at extinction were recorded for equivalence ratios ranging from a maximum of 0.9 to the lowest experimentally achievable equivalence ratio. The flame extinction limit for this volumetric-percentage of methane in the fuel-blend mixture was evaluated by extrapolating the data of percent-fuel in air-fuel mixture at zero-stretch. A graph of the flame extinction limits of the fuel-blend mixtures, ranging from the 0% to 100% methane in fuel mixtures shows the variation in flame-extinction characteristics of methane due to the addition of propane or ethane. The flame extinction limit for natural gas (Birmingham composition of 90% methane, 5% ethane and 5% nitrogen) was then determined.

Chapter IV

Results and Discussion

IV (a): Flame Appearances

Color images of methane-propane (80%-20% by volume) twin-flames at different volumetric flow rates are shown in Figures 4.1 and 4.2. For these particular set of images the nozzle separation was kept at 12 mm and volumetric flow rates were changed to vary the global stretch rate. During the inception stage of the twin-flames, the recorded images show a bright well-defined flame-boundary due to the fuel-rich mixture. A more diffusive flame-boundary was observed as the air-fuel mixture transits from fuel-rich to fuel-lean conditions. A gradual increase in the flame radius of curvature was noticed with an increasing air flow-rate. The images also confirm the insignificant wall effect on twin flames.

During the flame stretch process, the medium immediately adjacent to the flame front serves as a cold quenching medium. Under these stretched conditions, the flame is quenched due to a kind of non-adiabaticity caused either by the flame front curvature or by the velocity gradients. This quenching effect on the flame front leads to flame extinction. Figure 4.1 shows flames with an extinction stretch rate of 400 sec^{-1} whereas Figure 4.2 shows flames with an extinction rate of 800 sec^{-1} . The images in Figure 4.1 show no stress to increasing stretch rate (until extinction). The flame structures were better defined and more stable with higher air and fuel flow-rates, as seen in Figure 4.2. Twin-flames with lower stretch-rate are slightly green in color at the top burner, indicating the presence of high CH radical concentrations. Figures 4.3 and 4.4 show twin flame images of methane-propane fuel blend at 75%-25% mixture condition. Similar to

Figures 4.1 and 4.2, Figure 4.3 shows the flame images for a stretch rate of 400 sec^{-1} and Figure 4.4 shows the twin flame images for a stretch-rate of 800 sec^{-1} , respectively. Figure 4.5 and 4.6 show the twin-flame images for methane-ethane fuel blends with stretch-rates of 175 sec^{-1} and 250 sec^{-1} , respectively. It is interesting to note that even at low stretch-rates methane-ethane twin flames do not show any significant greenish region.

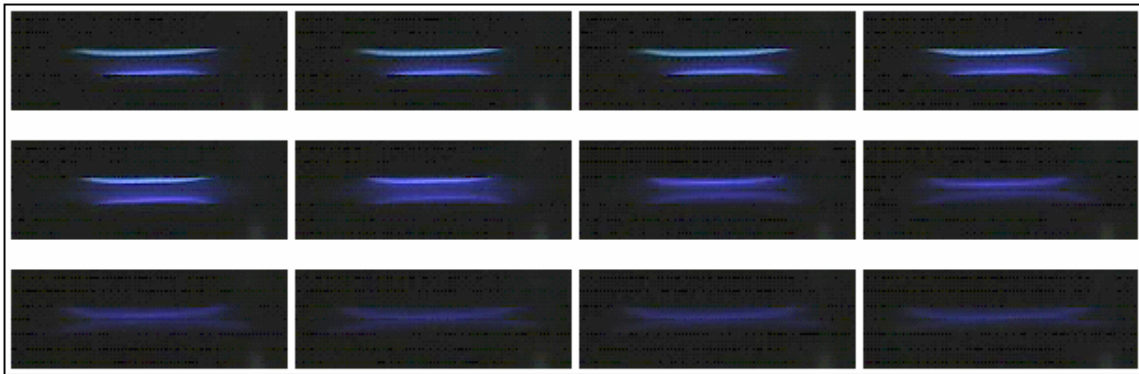


Figure 4.1: Twin-flame images of 80% CH_4 – 20% C_3H_8 fuel blend, from formation to just before extinction at a flame-stretch $\sim 400 \text{ sec}^{-1}$

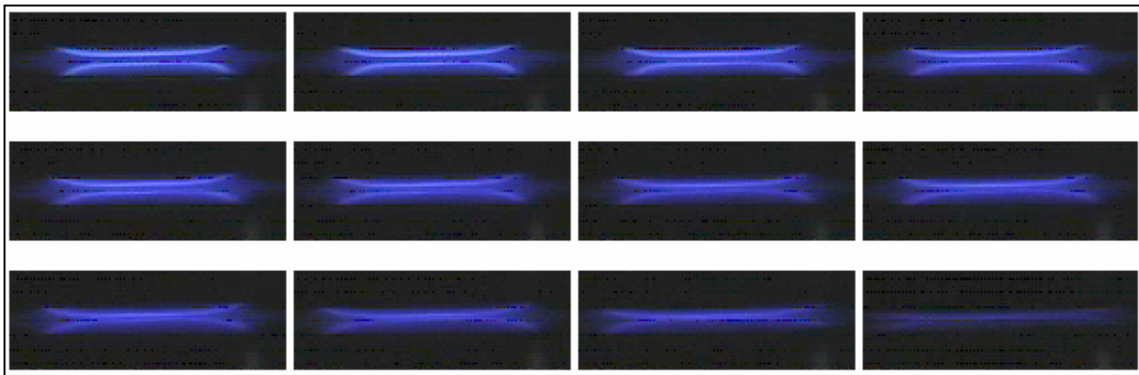


Figure 4.2: Twin-flame images of 80% CH_4 – 20% C_3H_8 fuel blend, from formation to just before extinction at a flame-stretch $\sim 800 \text{ sec}^{-1}$

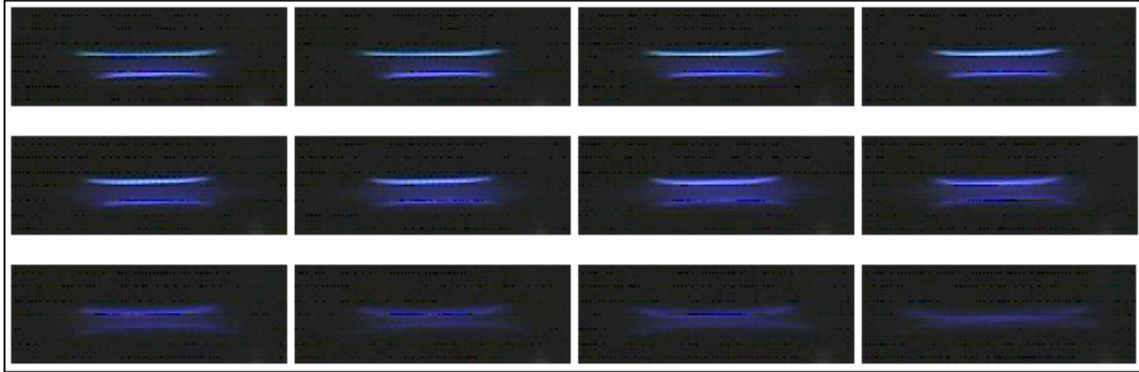


Figure 4.3: Twin-flame images of 75% CH_4 – 25% C_3H_8 fuel blend, from formation to just before extinction at a flame-stretch $\sim 400 \text{ sec}^{-1}$

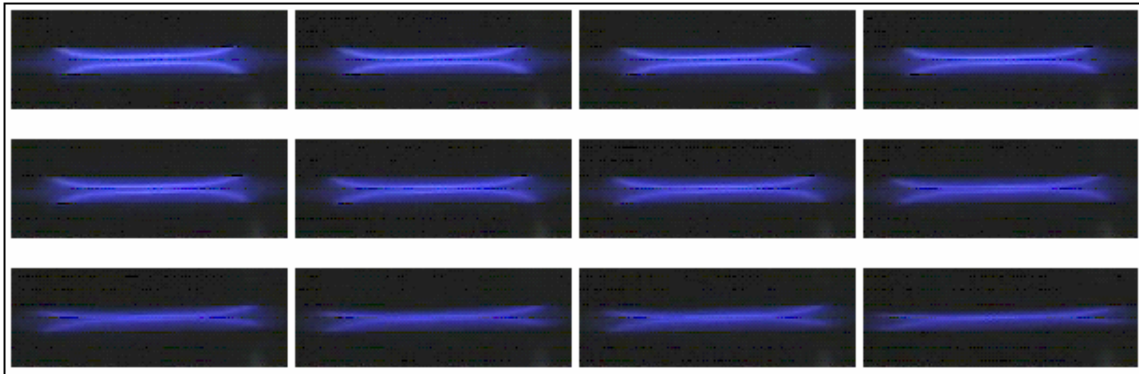


Figure 4.4: Twin-flame images of 75% CH_4 – 25% C_3H_8 fuel blend, from formation to just before extinction at a flame-stretch $\sim 800 \text{ sec}^{-1}$

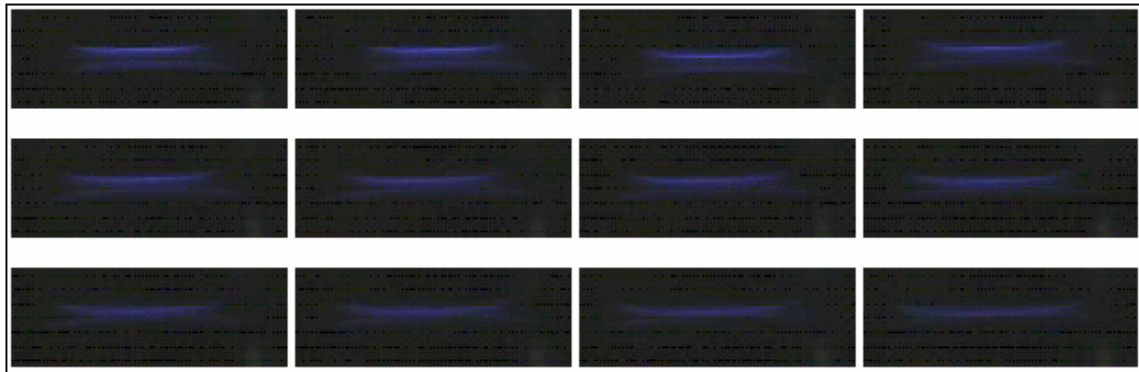


Figure 4.5: Twin-flame images of 93% CH_4 – 7% C_2H_6 fuel blend, from formation to just before extinction at a flame-stretch $\sim 175 \text{ sec}^{-1}$

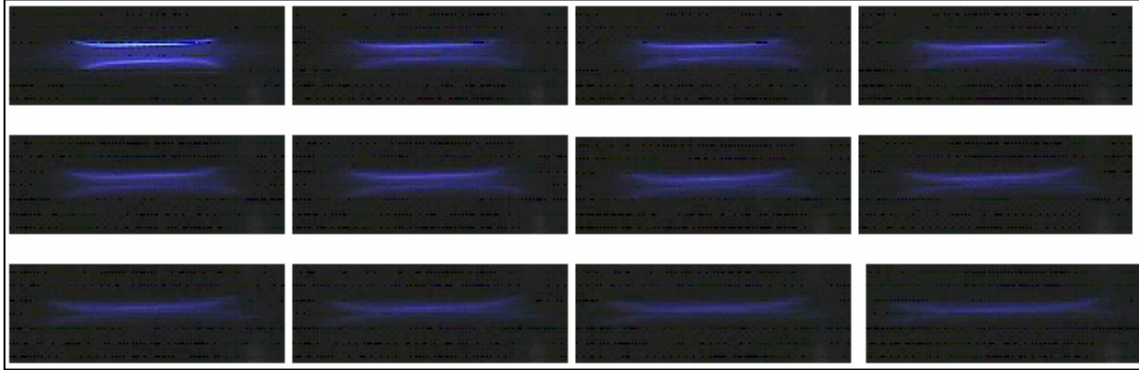


Figure 4.6: Twin-flame images of 93% CH₄ – 7% C₂H₆ fuel blend, from formation to just before extinction at a flame-stretch $\sim 250 \text{ sec}^{-1}$

IV (b): Flame Extinction:

IV.b.1: Pure fuels: 100% Methane and 100% Propane

Figure 4.7 and 4.8 show the extinction equivalence ratio (expressed as volumetric percent fuel in the air-fuel mixture, Appendix II) of methane and propane flames measured at different global stretch rates. The global stretch rate is defined as the ratio of nozzle exit velocity (U) and to half of the nozzle separation distance (d). The measured data are extrapolated (linearly) to obtain experimentally unattainable zero-stretch extinction conditions. The extinction equivalence ratio of methane and propane measured in the present study are 4.66% ($\Phi = 0.46$) and 2.25% ($\Phi = 0.51$) respectively. Table 4.1 summarizes the extinction value of methane and propane reported in past studies [Ishizuka and Law, 1982]. The flame extinction values measured in the present study are listed in the table and show an excellent agreement with previous measurements.

Author	Method	Flame Extinction Limits	
		% Methane	% Propane
Zabetakis	Propagating flame (tube)	5.00	2.10
Andrews and Bradley	Propagating flame (vessel)	4.50	-
Egerton and Thabet	Flat flame	5.10	2.01
Sorenson, Savage and Strehlow	Tent flame	4.00	-
Yamaoka and Tsuji	Double flame	4.70	-
Ishizuka and Law	Binary flame	4.80	2.00
Present Study	Twin flame	4.66	2.25

Table 4.1: Lower-flammability limits for methane and propane fuels [Source: Satoru, 1982]

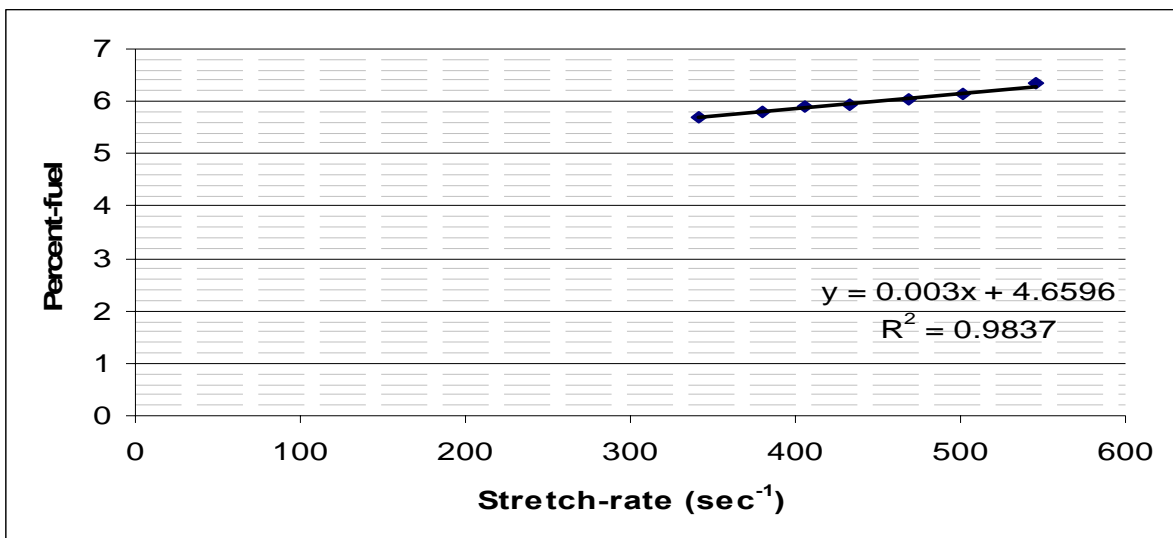


Figure 4.7: Flame extinction limit for 100% methane fuel

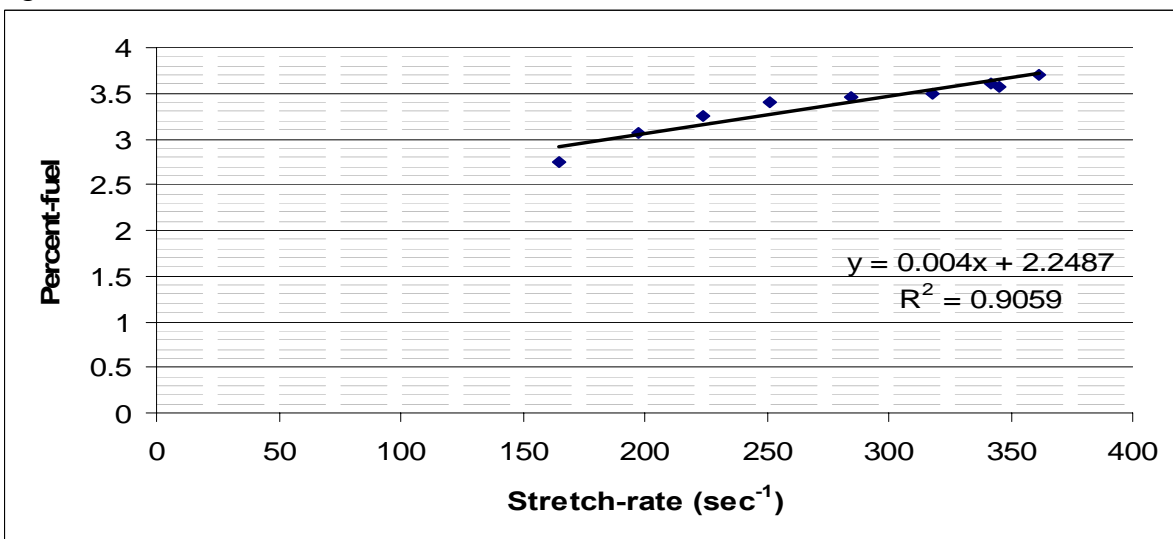


Figure 4.8: Flame extinction limit for 100% propane fuel

IV.b.2: Fuel Blends: Methane – Propane Blend

For different compositions of methane-propane fuel blend, lean extinction equivalence ratio (0.9 to the lowest experimentally attainable equivalence ratio) is measured at different stretch conditions. For each composition, data were repeated at least eight times to ensure the repeatability (and to compute the random error) of the measurements. Figure 4.9 through 4.14 show flame extinction limits of various methane-propane fuel-blend compositions at different stretch rates. The extrapolated zero-stretch values were obtained from the intercept of the linear curve fit of the extinction data.

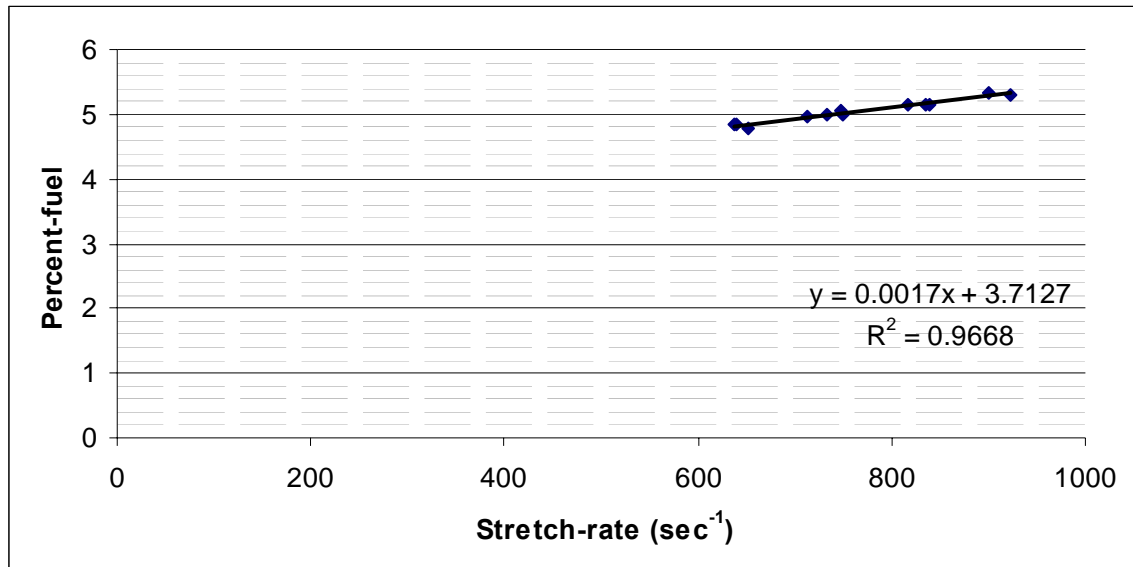


Figure 4.9: Flame extinction limit for 95% methane – 5% propane fuel-blend

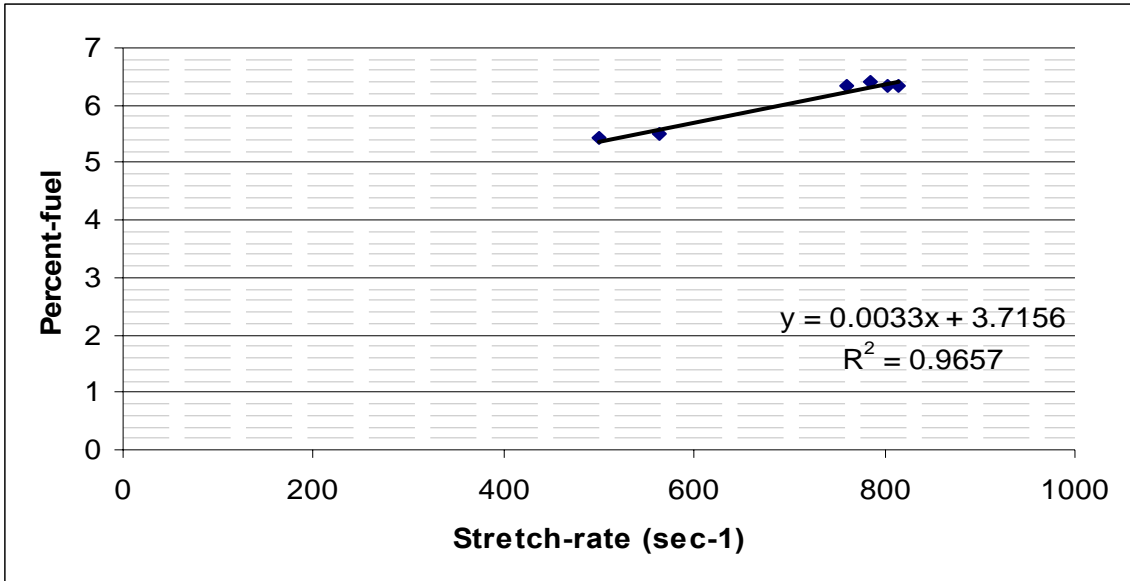


Figure 4.10: Flame extinction limit for 92% methane – 8% propane fuel-blend

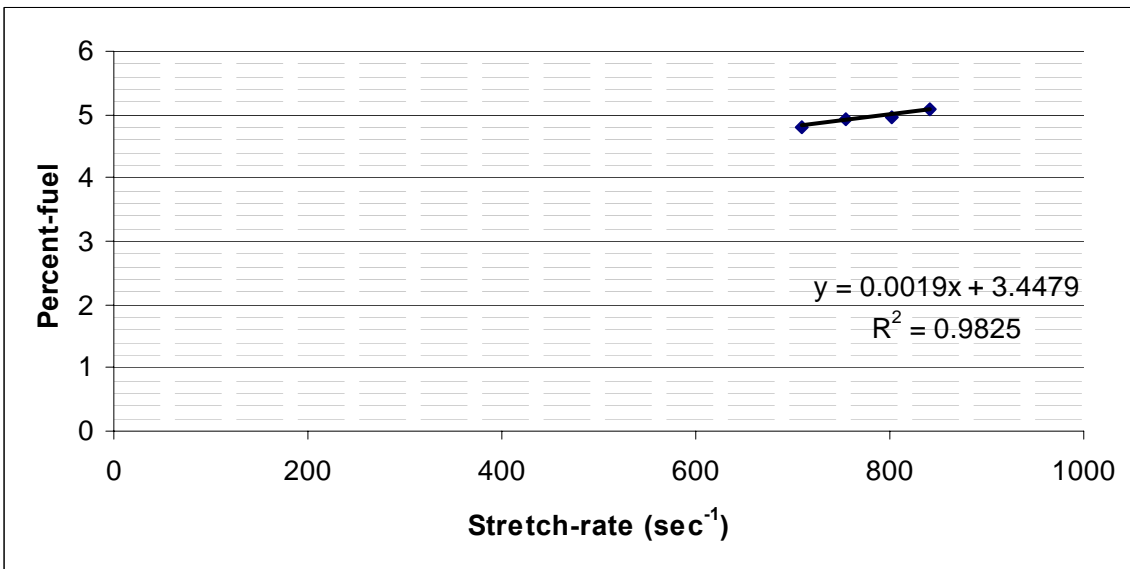


Figure 4.11: Flame extinction limit for 89% methane – 11% propane fuel-blend

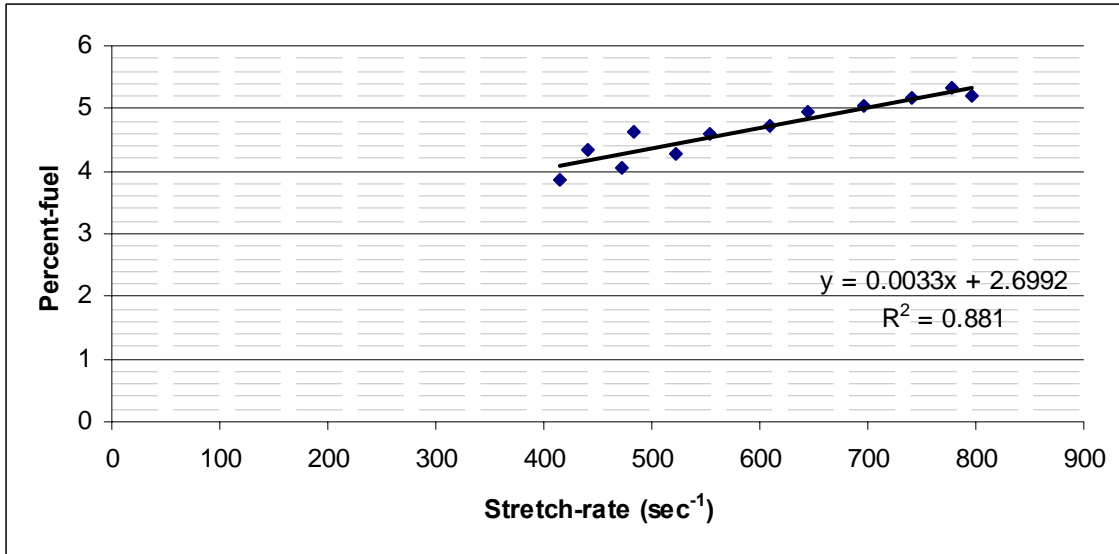


Figure 4.12: Flame extinction limit for 80% methane – 20% propane fuel-blend

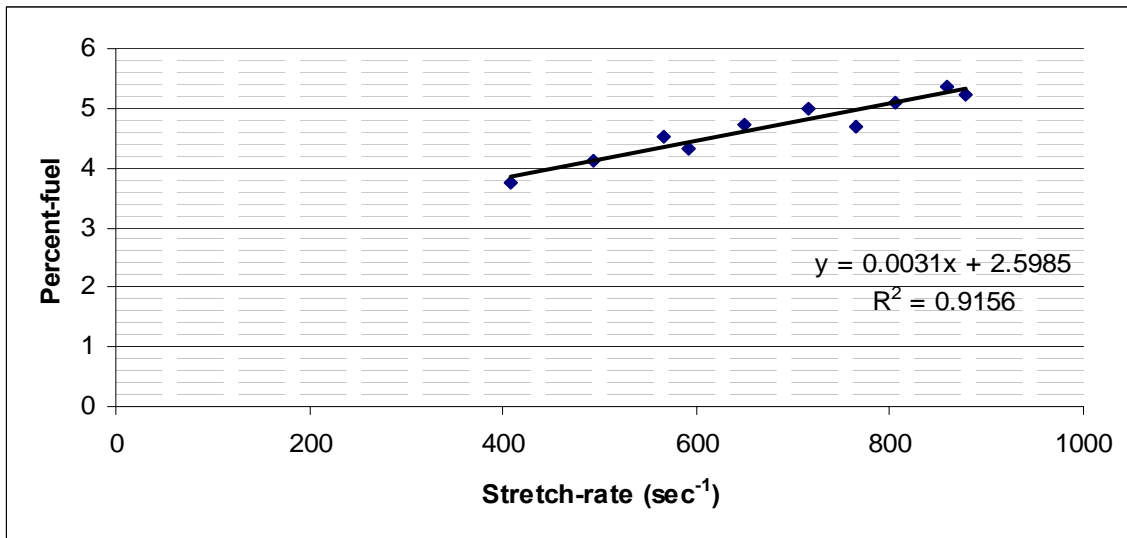


Figure 4.13: Flame extinction limit for 75% methane – 25% propane fuel-blend

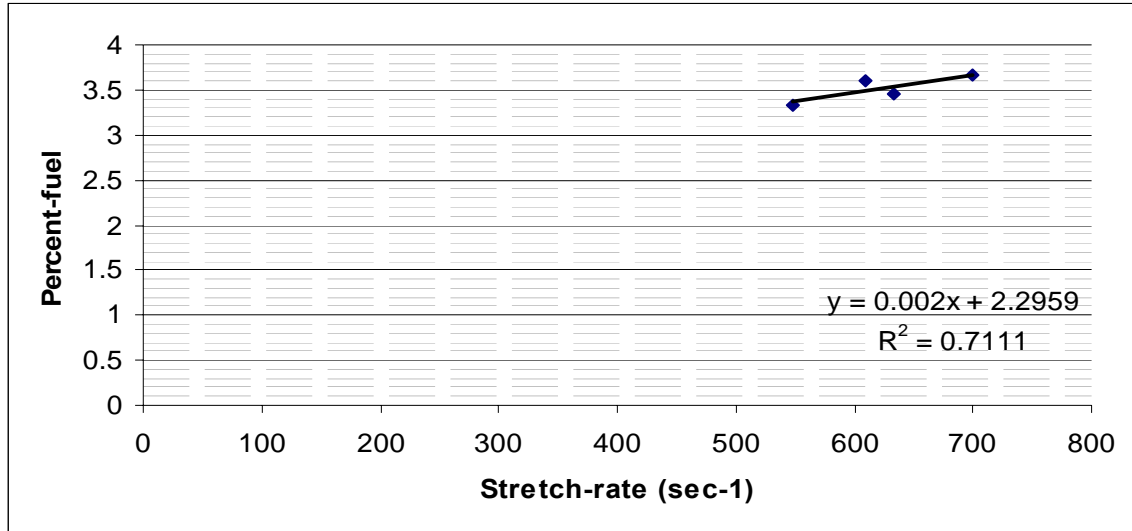


Figure 4.14: Flame extinction limit for 18% methane – 82% propane fuel-blend

Table 4.2 shows the two extinction points and their corresponding stretch rates which were used to deduce the zero-stretch extinction values (These are the two extreme points in above figures) at different compositions of methane-propane fuel blends.

%CH ₄ in CH ₄ -C ₃ H ₈ fuel blend	Lower point		Upper Point	
	stretch 'k'	% f _{ext}	stretch 'k'	% f _{ext}
100.00	341.77	5.70	545.16	6.34
95 – 5	636.94	4.84	922.72	5.30
92 – 8	499.94	5.43	814.04	6.33
89 – 11	710.24	4.82	891.53	5.11
86 – 14	578.18	5.99	755.63	6.38
80 – 20	414.38	3.85	797.22	5.20
75 – 25	409.16	3.75	877.52	5.25
18 – 82	548.62	3.33	699.81	3.66
0.00	165.15	2.75	361.24	3.70

Table 4.2: Lowest and highest fuel-percent in air-fuel mixture and its corresponding stretch-rates at extinction for methane-propane fuel blend

Figure 4.15 shows the zero-stretch flame extinction limits of methane-propane blended fuel flames as a function of methane concentrations in the fuel mixture. The flame extinction limits of methane-propane fuel blends show polynomial variations with the

methane concentration in the mixture. A polynomial regression technique was used to fit a curve through the points. The equation of the 5th order polynomial curve used to fit through the data points is as follows:

$$\%f_{ext} = (1.05 \times 10^{-9})f^5 - (1.3644 \times 10^{-7})f^4 + (6.40299 \times 10^{-6})f^3 - (1.2108459 \times 10^{-4})f^2 + (2.87305329 \times 10^{-3})f + 2.2483$$

This equation can be used to calculate the zero-stretch extinction limits of methane-propane fuel blends for a given concentration of methane in the mixture. The straight line in the figure represents the calculated values of flame extinction limits using Le Chatelier’s rule. It is evident that the Le Chatelier’s rule yields an erroneous prediction of flame extinction limits of methane-propane fuel blends.

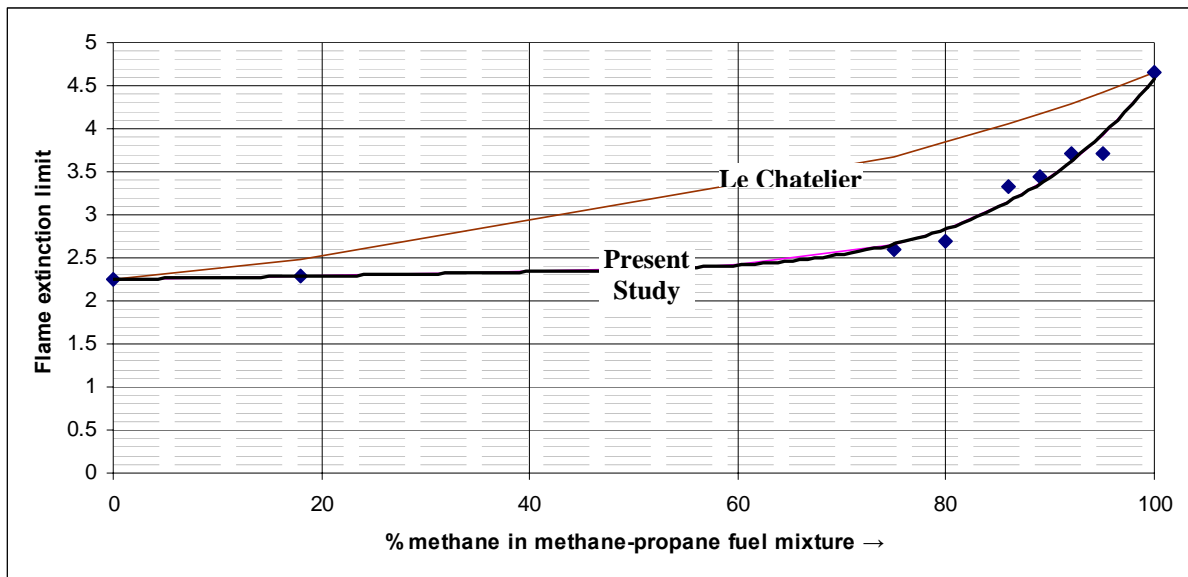


Figure 4.15: Trend of flame extinction limit of methane-propane fuel-blends, experimental data in comparison with values predicted by Le Chatelier rule

The error between the predicted flame extinction limit using the fifth-order polynomial and the experimental results are less than 6% for the methane-propane fuel blend matrix. Table 4.3 shows the comparison between the experimental flame

extinction limits for methane-propane fuel blends, values predicted by the polynomial equation and values calculated using the Le Chatelier's rule.

% Methane	Exptl. Value	Predicted value			Le Chatelier's value		
	F.E Limit	F.E Limit	Error	% Error	F.E Limit	Error	% Error
0.000	2.249	2.248	0.000	0.018	2.249	0.000	0.000
18.000	2.296	2.286	0.010	0.441	2.480	0.184	8.003
75.000	2.599	2.659	0.060	2.312	3.675	1.076	41.415
80.000	2.699	2.834	0.134	4.979	3.837	1.138	42.149
86.000	3.319	3.149	0.171	5.143	4.051	0.732	22.058
89.000	3.448	3.362	0.086	2.506	4.168	0.720	20.886
92.000	3.716	3.620	0.096	2.584	4.292	0.576	15.500
95.000	3.713	3.930	0.217	5.847	4.423	0.710	19.119
100.000	4.660	4.584	0.076	1.628	4.660	0.000	0.000

Table 4.3: Comparison of flame extinction limits obtained experimentally, value predicted by fifth-order polynomial and calculated by Le Chatelier's rule

IV.b.3: Fuel Blend: Methane-Ethane Blend

Figures 4.16 to 4.20 show the flame extinction data measured at different global stretch rates for various methane-ethane fuel compositions. The extrapolated zero-stretch values obtained from linear curve fits are also shown in the same figures.

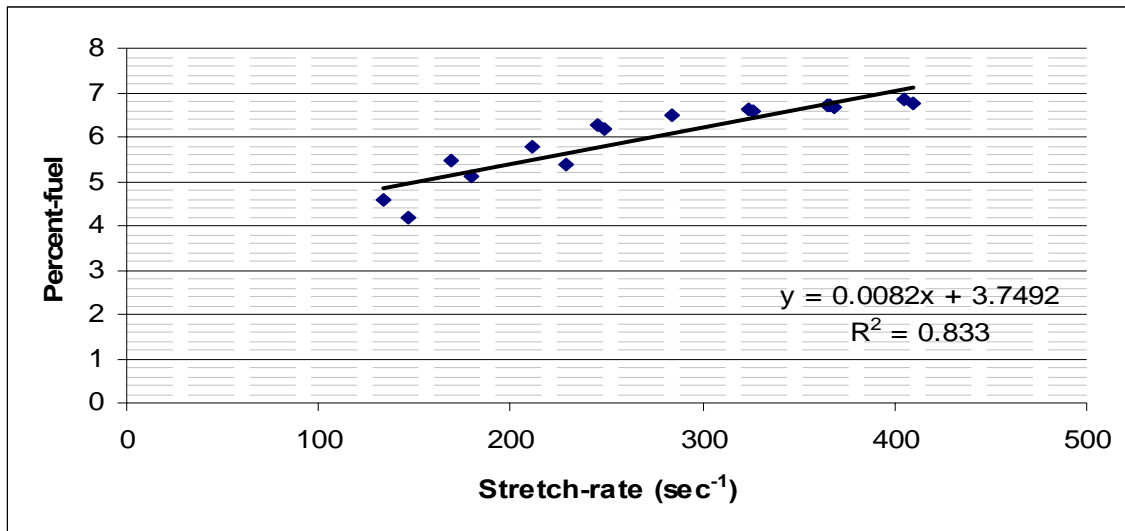


Figure 4.16: Flame extinction limit for 93% methane – 7% ethane fuel-blend

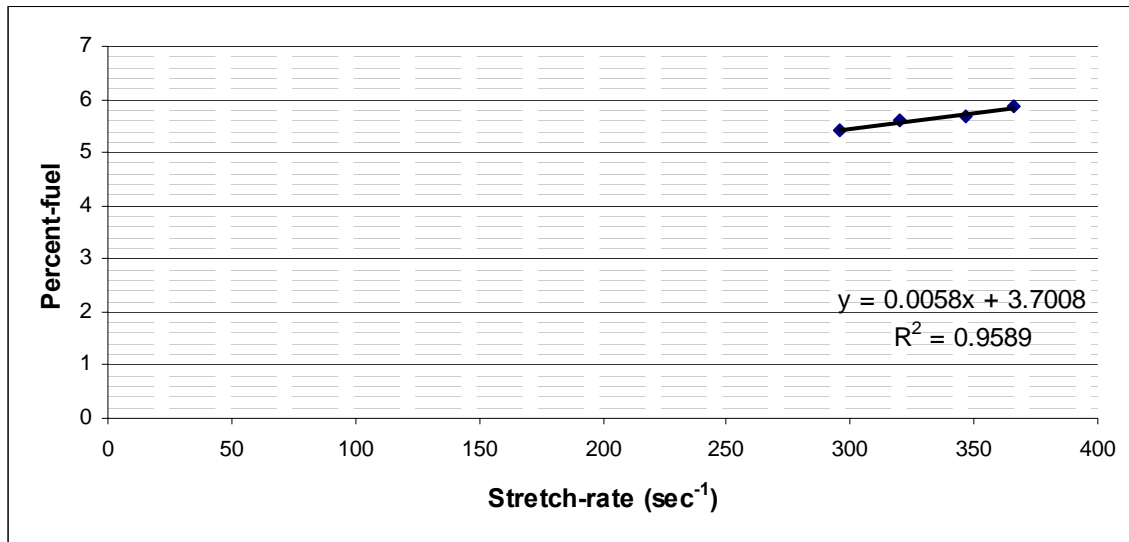


Figure 4.17: Flame extinction limit for 90% methane – 10% ethane fuel-blend

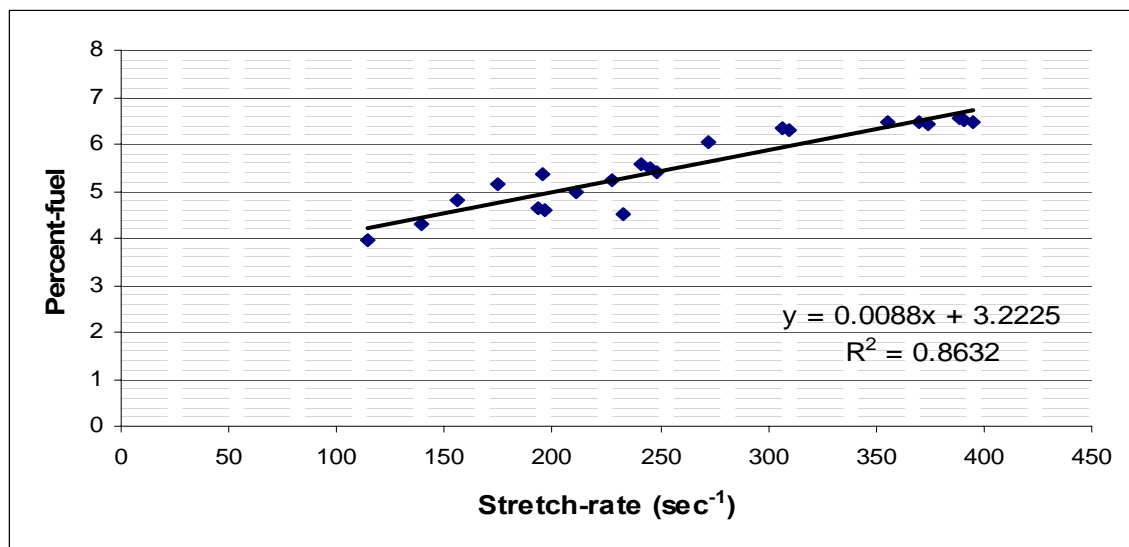


Figure 4.18: Flame extinction limit for 85% methane – 15% ethane fuel-blend

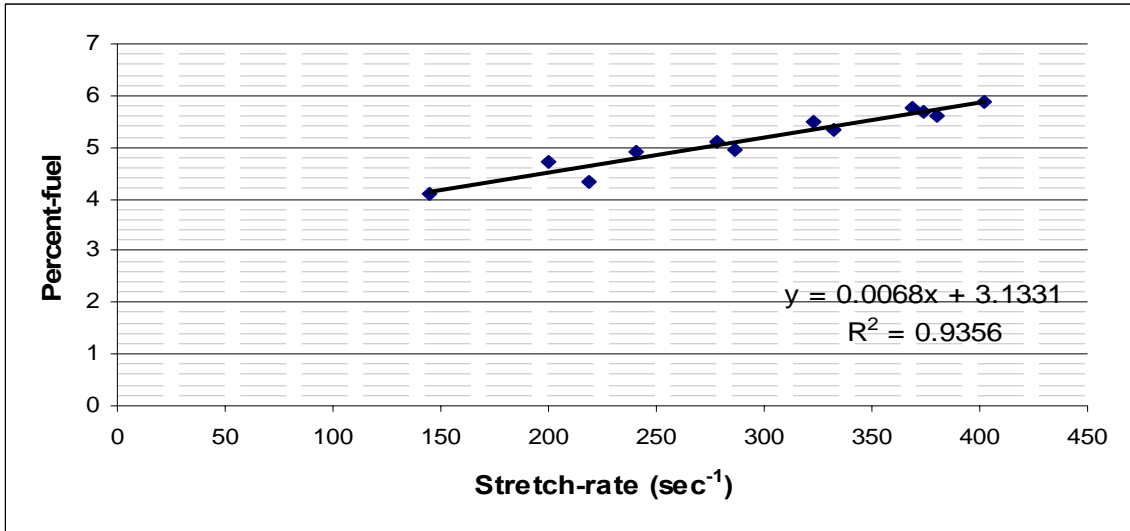


Figure 4.19: Flame extinction limit for 81% methane – 19% ethane fuel-blend

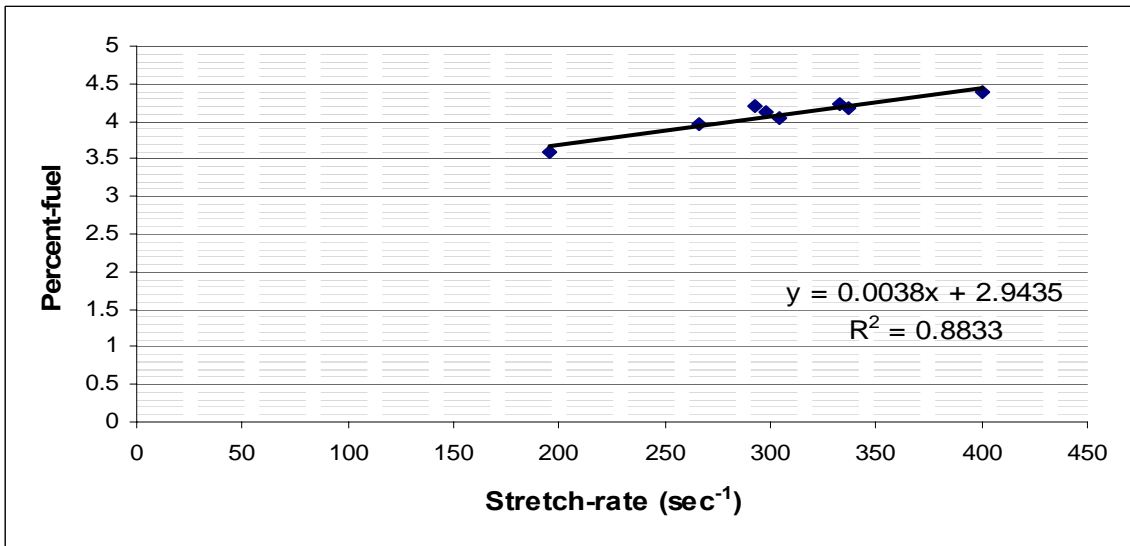


Figure 4.20: Flame extinction limit for 20% methane – 80% ethane fuel-blend

Table 4.4 shows the two extreme extinction points and their corresponding stretch rates which were used to deduce the zero-stretch extinction of methane-ethane blended fuel flames.

% CH ₄ in CH ₄ -C ₂ H ₆ fuel blend	Lower Point		Upper Point	
	Stretch 'k'	% f	Stretch 'k'	% f
100.00	341.77	5.70	545.16	6.34
93-7	134.24	4.57	409.93	6.74
90-10	296.13	5.42	366.46	5.87
85-15	113.89	3.94	394.67	6.45
81-19	144.83	4.08	401.89	5.89
20-80	195.65	3.59	400.46	4.38

Table 4.4: Lowest and highest fuel-percent in air-fuel mixture and its corresponding stretch-rates at extinction for methane-ethane fuel blend

Figure 4.21 shows the zero-stretch flame extinction limits of methane-ethane blended fuel flames as a function of methane concentrations in the fuel mixture. Similar to the methane-propane blend, a fifth order polynomial best defines the relation between the zero-stretch flame extinction limit and methane concentration in methane-ethane mixtures.

$$\%f_{ext} = (2.1 \times 10^{-9})f^5 - (3.5752 \times 10^{-7})f^4 + (2.095425 \times 10^{-5})f^3 - (5.037353 \times 10^{-4})f^2 + 6.08980409f + 2.8923$$

Figure 4.21 also shows the calculated flame extinction limits of methane-ethane blends using the Le Chatelier's rule. The Le Chatelier prediction shows very poor agreement with experimental measurements.

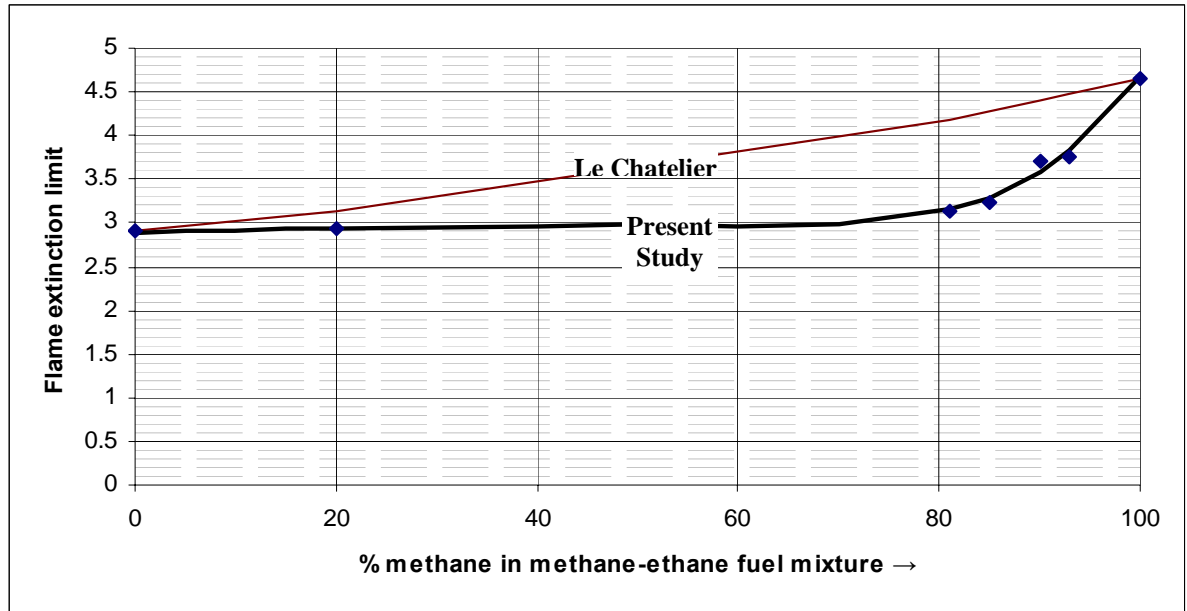


Figure 4.21: Trend of flame extinction limit of methane-ethane fuel-blends, experimental data in comparison with values predicted by Le Chatelier rule

Table 4.5 shows a comparison between the experimentally obtained flame extinction limit, the flame extinction limits obtained by using the fifth order polynomial and the flame extinction values calculated using the Le Chatelier's rule. The error in predicted flame extinction limit using the fifth order polynomial stays within 5% of the experimentally obtained flame extinction limit. However, the discrepancy between the experimental measurements and Le Chatelier calculations are as high as 35% at some mixture compositions.

% Methane	Exptl. Value	Predicted Value			Le Chatelier Value		
	F.E Limit	F.E Limit	Error	% Error	F.E Limit	Error	% Error
0.000	2.900	2.892	0.008	0.265	2.900	0.000	0.000
20.000	2.944	2.930	0.014	0.467	3.137	0.193	6.571
81.000	3.133	3.149	0.016	0.498	4.178	1.045	33.349
85.000	3.223	3.294	0.072	2.220	4.271	1.048	32.533
90.000	3.701	3.579	0.122	3.286	4.393	0.692	18.705
93.000	3.749	3.822	0.072	1.933	4.470	0.721	19.219
100.000	4.660	4.666	0.007	0.141	4.660	0.000	0.000

Table 4.5: Comparison of flame extinction limits obtained experimentally, value predicted by fifth-order polynomial and calculated by Le Chatelier's rule

IV.b.4: Natural Gas Composition

A natural gas composition of 90% methane, 5% ethane and 5% nitrogen (the Birmingham composition) was also investigated to extend the present the study to commercial fuels. Figure 4.22 shows the flame extinction limit ($f_{\text{ext}} = 3.62\%$) obtained at different stretch rates for the Birmingham fuel composition. The zero-stretch extinction limit for this particular natural gas composition is 3.62 % which is comparable to the extinction limits (3.701%) of 90-10% methane-ethane mixtures. It appears that the effects of nitrogen insignificant at this composition level.

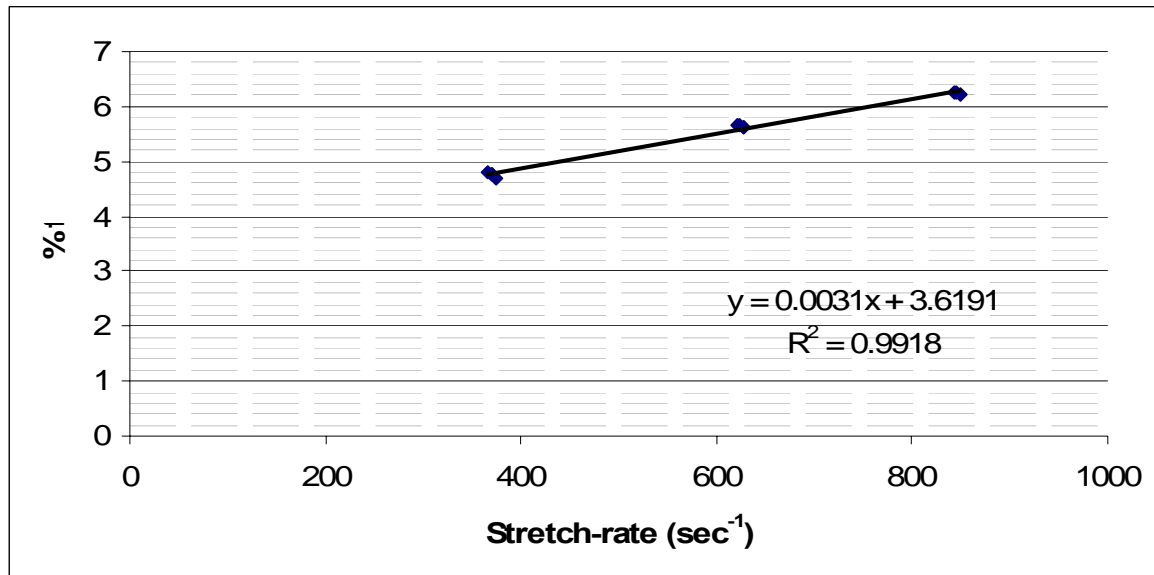


Figure 4.22: Flame extinction limit for Birmingham fuel composition of 90% CH₄, 5% C₂H₆ and 5% N₂

Chapter V

Conclusions and Recommendations

V.a. General Remarks

The lean extinction characteristics of methane-propane and methane-ethane fuel blends have been presented in this report. The flame extinction limits of pure fuels (i.e. methane and propane) were also measured to validate the experimental setup and methodologies. The primary objective of this project was to develop a relation between the extinction limits and the compositions of binary fuel blends. In addition, the present study also analyzed the accuracy of Le Chatelier rule for the prediction of the extinction limits for fuel blends.

Natural gas compositions significantly affect the emission and operational performances of natural gas turbine combustors. Designers of gas turbine combustors of advanced power systems have goals to achieve very low plant emissions (NO_x less than 2-ppm), fuel variability, and fuel flexibility. The variation in fuel properties may cause a “well-tuned,” low NO_x, LP or LPP gas turbine to suffer significant operational and performance penalties. Although a considerable amount of research has been done on flame extinction characteristics of pure fuels, the synergetic relation between the compositions and flame extinction of fuel blends such as natural gas and syngas are largely unknown. With an emerging need to address gas turbine combustor issues such as ultra-low emission, fuel variability and fuel flexibility, fundamental information and data regarding the combustion characteristics of natural gas and alternative fuels are essential. The research was aimed at addressing fuel compositions issue and the flame extinction

behavior of natural gas. The primary goal for this research project was to understand the effects of compositions on the extinction behavior of various constituents of natural gas. The project used laboratory experiments to generate flame extinction maps of hydrocarbon fuel blends with different compositions. The outcomes of the project will enable design of natural gas fueled gas turbine combustors with improved stability and emissions.

The flame extinction limit of the fuel blends varied in between the extinction limits of the individual fuels. However, the relation between the flame extinction limit and the compositions of blended fuels are not linear as indicated by the Le Chatelier's rule. It was found that the trend of the flame extinction limits for methane-propane and methane-ethane fuel blends are best defined by fifth-order polynomials.

V.b. Conclusions

In the present study the measurements of flame extinction limits of methane-propane and methane-ethane fuel blends lead to the following results.

1. The flame extinction limits of methane-propane and methane-ethane fuel blends have a polynomial relation with the concentration of component fuels in the mixture.
2. The discrepancy between the experimental measurements and Le Chatelier calculations are as high as 35% at some compositions of methane-propane and methane-ethane fuel blends.
3. The experimentally determined polynomial relations between the flame extinction limits of methane-propane blends and the methane concentration in the mixture is:

$$\%f_{ext} = (1.05 \times 10^{-9})f^5 - (1.3644 \times 10^{-7})f^4 + (6.40299 \times 10^{-6})f^3 - (1.2108459 \times 10^{-4})f^2 + (2.87305329 \times 10^{-3})f + 2.2483$$

4. The experimentally determined polynomial relations between the flame extinction limits of methane-ethane blends and the methane concentration in the mixture is:

$$\%f_{ext} = (2.1 \times 10^{-9})f^5 - (3.5752 \times 10^{-7})f^4 + (2.095425 \times 10^{-5})f^3 - (5.037353 \times 10^{-4})f^2 + 6.08980409 f + 2.8923$$

5. The zero-stretch extinction limit of the Birmingham natural gas is 3.62 %.

V.c. Recommendations and Future Research

A further study on hydrocarbon blended fuel flames to study the formation of intermediate radical concentration will be beneficial to explain some of the results present in this report. In addition, a numerical investigation to identify the contribution of loss mechanism on the extinction behavior of fuel blends will certainly broaden the scope of the current project.

Bibliography:

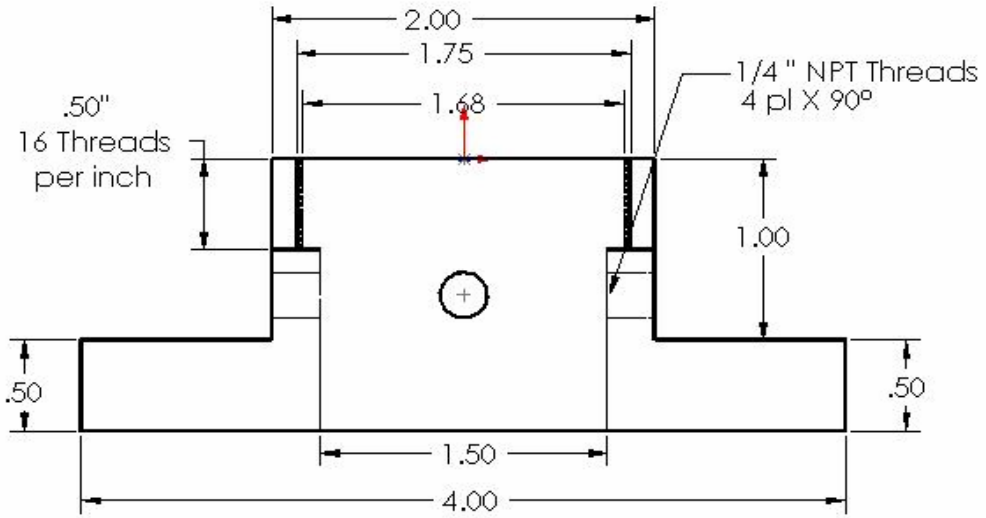
- Abbud-Madrid, A. and Ronney, P. D., "Premixed Flame Propagation in an Optically-thick Gas", *AIAA Journal*, 31:2179-2181(1993).
- Broad Agency Announcement For Contracts, Grants, Cooperative Agreements, And Other Transactions Army Research Laboratory, U. S. Department Of Army Research Triangle Park, NC 27709-2211, DAAD19-00-R-0010, (July 2000-2003).
- Bui-Pham, M. N., Lutz, A. E., Miller, J. A., Desjardin, M., O'Shaughnessy, D. M., and Zondlak, R. J., "Rich Flammability Limits in CH₃OH/CO/diluent Mixtures", *Combustion Science and Technology*, 109:71-91(1995),
- Choudhuri, A. R. and Gollahalli, S. R., "Combustion Characteristics of Hydrogen-Hydrogen Hybrid Fuel", *International Journal of Hydrogen Energy*, 25:451-462 (2000)
- Choudhuri A. R. and Gollahalli, S.R."Intermediate Radical Concentrations in Hydrogen-Natural Gas Blended Fuel Jet Flames," *International Journal of Hydrogen Energy*, 29:1293-1302 (2004).
- Choudhuri A. R. and Gollahalli, S.R. "Stability of Hydrogen-Hydrocarbon Blended Fuel Flames," *AIAA Journal of Propulsion and Power*, 19, (2): 220-225 (2003a).
- Choudhuri A. R. and Gollahalli, S.R. "Global Characteristics of Hydrogen-Hydrocarbon Composite Fuel Turbulent Jet Flames," *International Journal of Hydrogen Energy*, 28:445-454(2003b).
- Choudhuri A. R. and Gollahalli, S.R, "Laser Induced Fluorescence Measurements of Radical Concentrations in Hydrogen-Hydrocarbon Blended Gas Fuel Flames," *International Journal of Hydrogen Energy*, 25:1119-1127(2000a).
- Choudhuri A. R. and Gollahalli, S.R., "Combustion Characteristics of Hydrogen-Hydrocarbon Hybrid Fuel," *International Journal of Hydrogen Energy*, 25: 451-462 (2000b).
- Coward, H.F., and Jones, G. W., *Limits of Flammability of Gases and Vapors*, Bulletin 503, Bureau of Mines (1952).
- Egolfopoulos, F.N., Law, C. K., "An Experimental and Computational Study of the Burning Rates of Ultra-Lean to Moderately-Rich H₂/O₂/N₂ Laminar Flames with Pressure Variations", *Proceedings of Combustion Institute*, 23:413-421 (1990).
- El-sherif, A.S., "Effects of Natural Gas Composition on the Nitrogen Oxide, Flame Structure and Burning Velocity Under Laminar Premixed Flame Conditions", *Fuel*, 77(14): 1539-1546 (1998).
- Frenklach, M., Wang, H., Goldenberg, M., Smith, G. P., Golden, D. M., Bowman, C. T., Hanson, R. K., Gardiner, W. C., and Lissianski, V., *GRI-Mech-An Optimized Detailed Chemical Reaction Mechanism for Methane Combustion*, Gas Research Institute Topical Report, Report No. GRI-95/0058 (1995).
- Giovangigli, V. and Smooke, M. "Application of Continuation Methods to Plane Premixed Laminar Flames", *Combustion Science and Technology*, 87:241-256 (1992).
- Golovitchev, V. I., and Bruno, C., "Numerical Study of the Ignition of Silane/Hydrogen Mixtures", *Journal of Propulsion and Power*, 15(1):82-91(1999).

- Hertzberg, M., *The Theory of Flammability Limits, Natural Convection*. Bulletin 8127, Bureau of Mines (1976).
- Ishizuka and Law, “An Experimental Study on Extinction and Stability of Stretched Premixed Flames,” *Nineteenth Symposium(International) on Combustion, The Combustion Institute*, 327-335 (1982)
- Lakshmisha, K. N., Paul, P. J., and Mukundu, H. S., “On the Flammability Limit and Heat Loss in Flames with detailed Chemistry”, *Proceedings of Combustion Institute*, 23:433-440 (1990).
- Law, C. K. and Egolfopoulos, “Chain Mechanisms in the overall Reaction Orders in Laminar Flame Propagation”, *Twenty-Third Symposium(International) on Combustion, The Combustion Institute*, 109:413-420-873 (1990).
- Lewis, B. and von Elbe, G., *Combustion, Flames, and Explosion of Gases*, 3rd edition, Academic Press, Orlando, (1987).
- Pfahl, U. J., Ross, M. C., Shepherd, J. E., Pasamehmetoglu, K. O., and Unal, C., “Flammability Limits, Ignition Energy and Flame Speeds in Hydrogen-Methane-Ammonia-Nitrous Oxide-Oxygen-Nitrogen Mixtures”, *Combustion and Flame*, 123:140-158 (2000).
- Pitts, W. M., “Importance of Isothermal Mixing Processes to the understanding of Lift-off and Blowout of Turbulent Jet Diffusion Flames”, *Combustion and Flame*, 76: 197-212 (1989).
- Ronney, P. D. “Premixed-Gas Flames”, *Microgravity Combustion: Fire in Free Fall*, 35-82 (2001).
- Ronney, P. D., “Effect of Gravity on Laminar Premixed Gas Combustion II: Ignition and Extinction Phenomena”, *Combustion and Flame*, 62: 121-133 (1985)
- Spalding, D. B., “Classical Theory of Flame Extinction by Heat Loss”, *Proceedings Royal Society (London), Series A*, 240:83-100 (1957).
- Sung, C. J. and Law, C. K., “Extinction Mechanisms of Near-Limit Premixed Flames and Extended Limits of Flammability”, *Twenty-Sixth Symposium of Combustion, The Combustion Institute*, 25:865-873 (1996).
- Sung, C. J., Huang, Y. and Eng, J. A., “Effects of Reformer Gas Addition on the Laminar Flame Speeds and Flammability Limits of n-Butane and Iso-butane Flames”, *Combustion and Flame*, 126:1699-1713 (2001).
- Tanord, C., and Pease, R. N., *Journal of Chemical Physics*, 15:431(1947).
- Yu, G., Law, C. K., and Wu, C. K., “Laminar Flame Speeds of Hydrocarbon + Air Mixtures with Hydrogen Addition”, *Combustion and Flame*, 63:339-347 (1986).

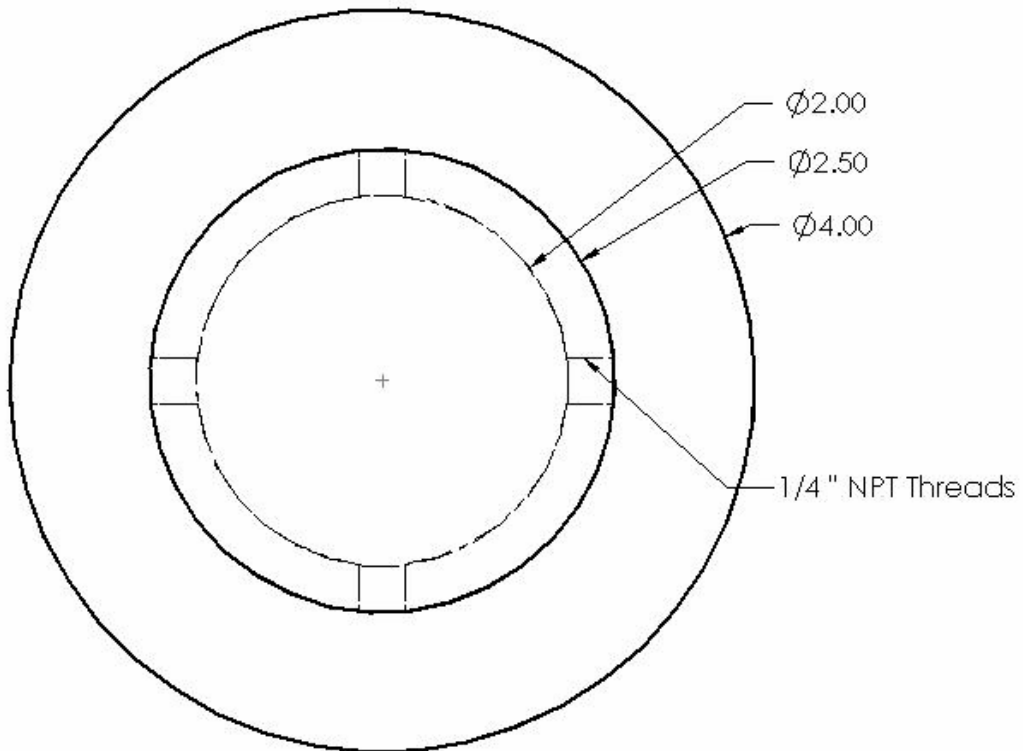
APPENDIX I: CAD Drawings

Manifold

Front View

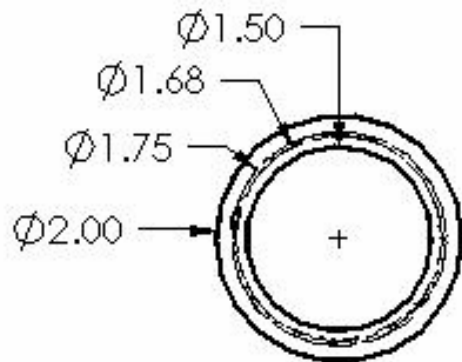
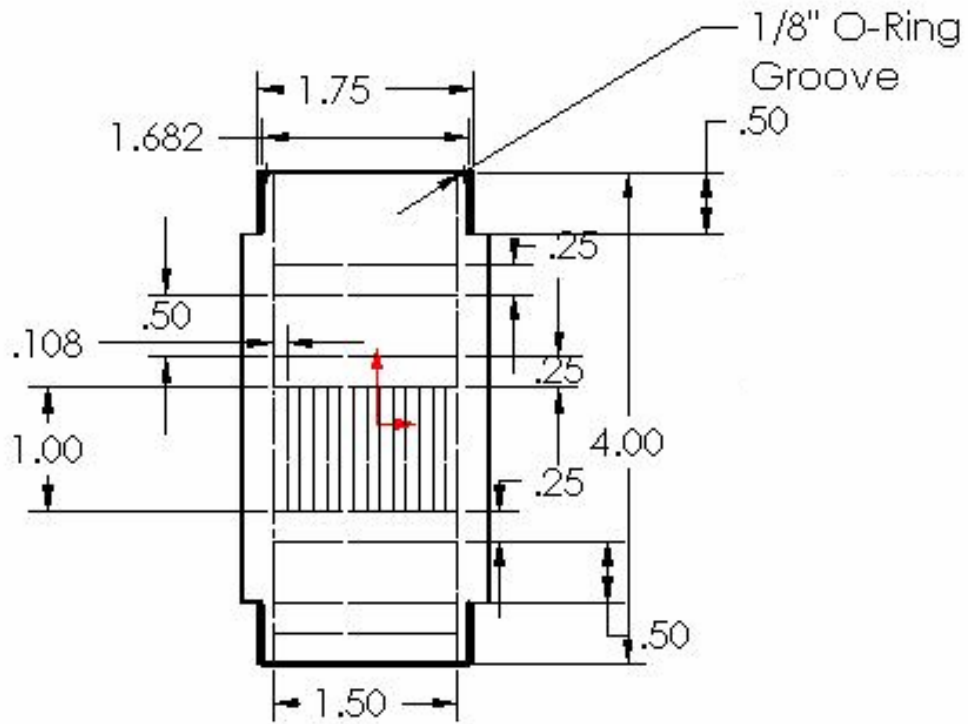


Top View



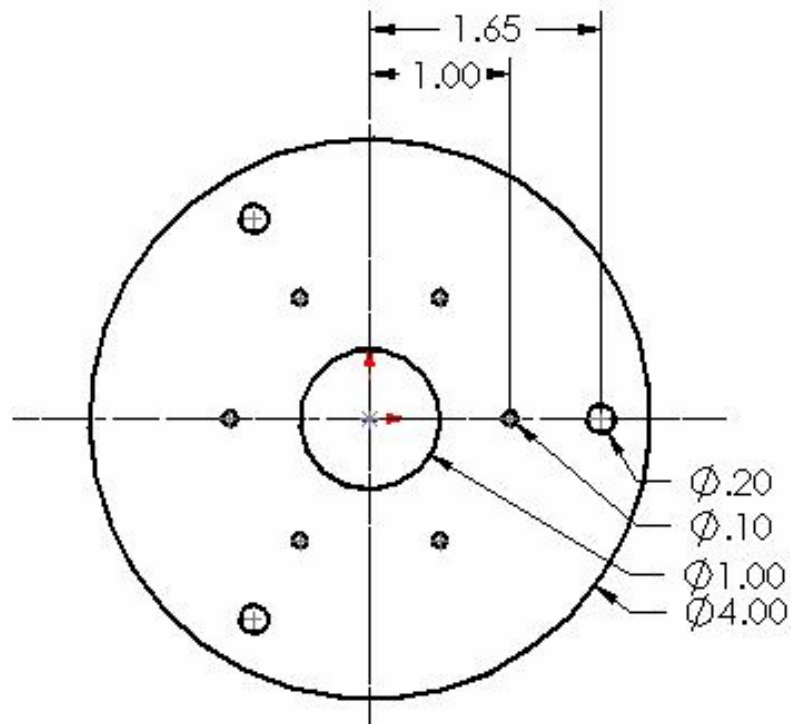
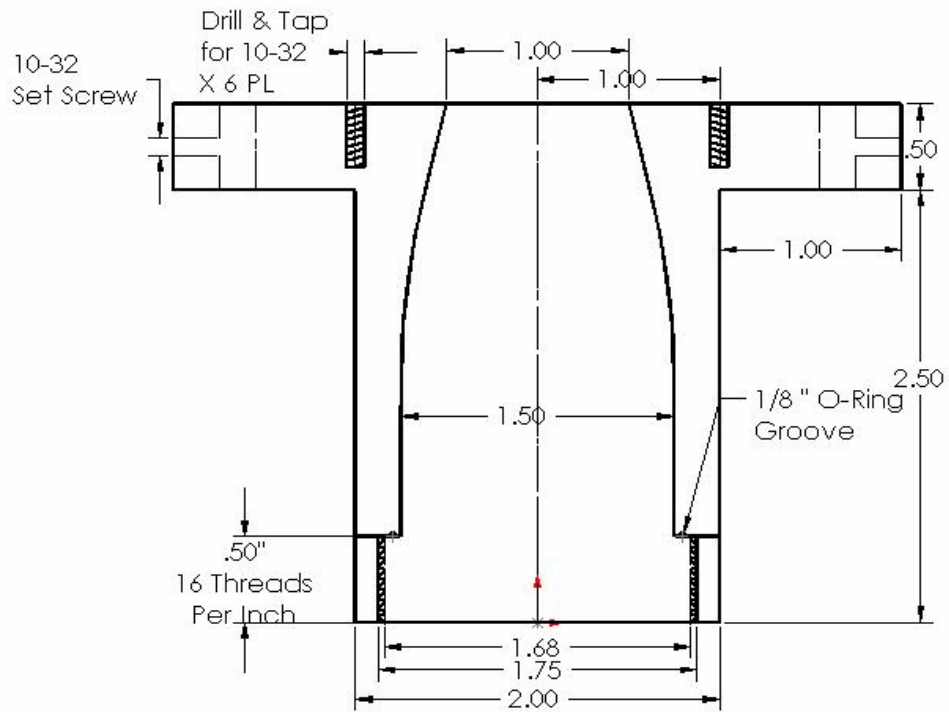
Stem

Front View and Top View



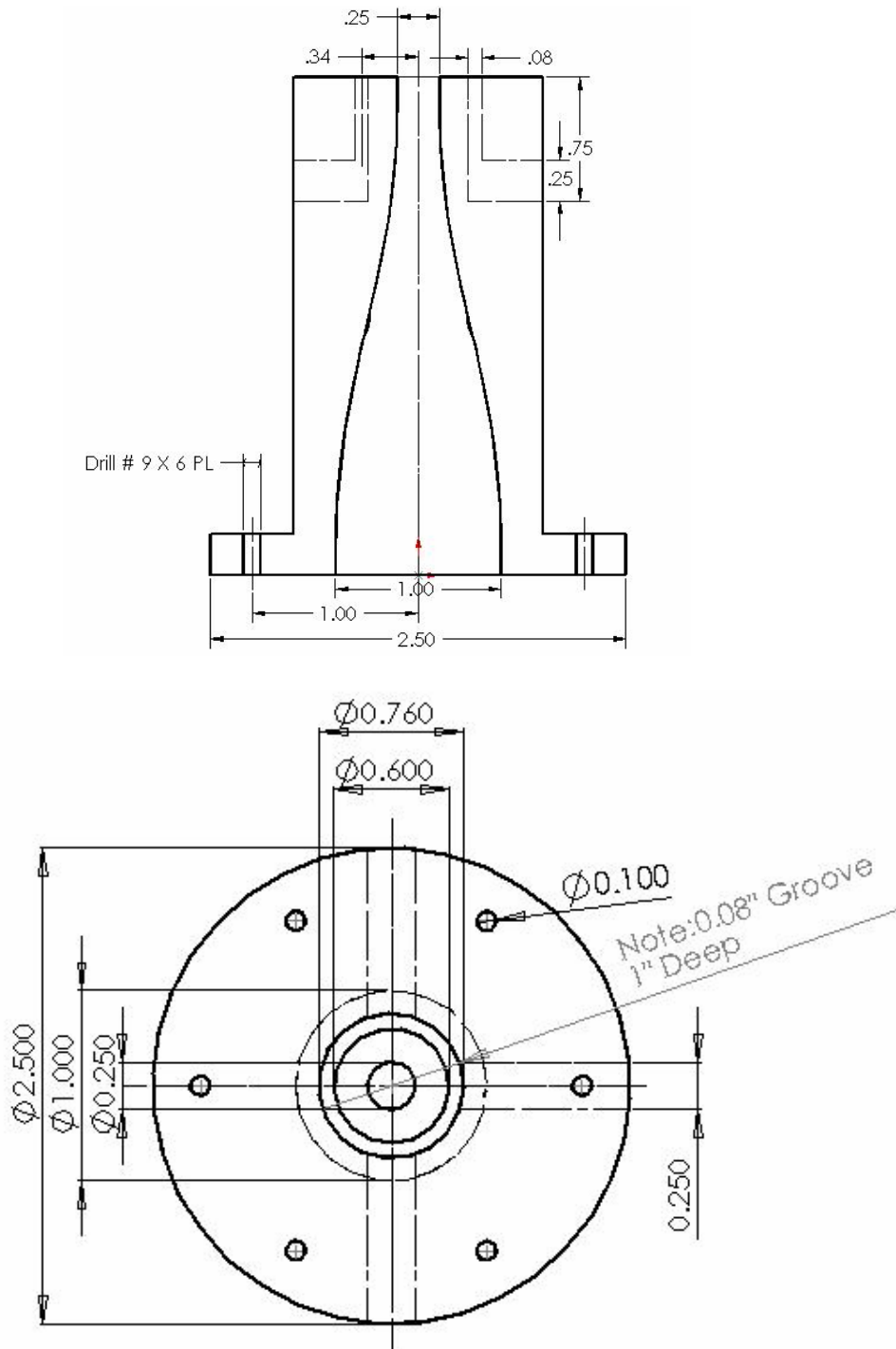
Connector

Front View and Top View



Nozzle

Front View and Top View



APPENDIX II: Conversion of Equivalence Ratio to %-fuel and vice-versa

Example 1: Consider an air-ethane fuel mixture, with Equivalence ratio $\Phi = 0.5$, the corresponding percentage of the fuel in mixture is:

$$(A/F)_{act} = \frac{(A/F)_{stoic}}{\Phi} \times \frac{\text{mol. wt. of } C_2H_6}{\text{mol. wt. of air}}$$

$$(A/F)_{act} = \frac{15.9846}{0.5} \times \frac{30.069}{28.85}$$

$$(A/F)_{act} = 33.32$$

$$\therefore \% \text{ fuel} = \frac{1}{(A/F)_{act} + 1} \times 100$$

$$\% \text{ fuel} = \frac{1}{34.32} \times 100 = 2.1\%$$

Example 2: Consider the given mixture has 2.1% of ethane in the ethane-air mixture, its corresponding equivalence ratio is:

$$(A/F)_{act} = \frac{\% \text{ air in mixture}}{\% \text{ fuel in mixture}} \times \frac{\text{mol. wt. of air}}{\text{mol. wt. of } C_2H_6}$$

$$(A/F)_{act} = \frac{0.979 \times 28.85}{0.021 \times 44.096} = 30.5$$

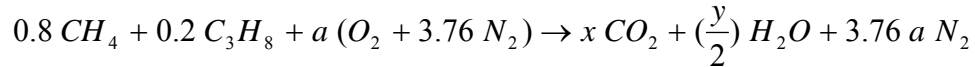
$$\therefore \Phi = \frac{(A/F)_{stoic}}{(A/F)_{act}} = \frac{15.57}{30.5}$$

$$\Phi = 0.51$$

APPENDIX III: Air-fuel Stoichiometric ratio for fuel blends

Example 1: Consider a fuel blend of 80% CH₄ and 20% C₃H₈; the stoichiometric ratio of the air-fuel mixture is:

Chemical reaction:



where, $x = \text{no. of carbon atoms in the reaction}$

$y = \text{no. of hydrogen atoms in the reaction}$

$$a = x + \frac{y}{4}$$

Number of carbon atoms in the reaction: x

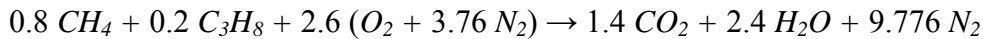
$$C: 0.8 + (0.2 \times 3) = 1.4$$

Number of hydrogen atoms in the reaction: y

$$H: (0.8 \times 4) + (0.2 \times 8) = 4.8$$

$$\therefore a = 1.4 + \left(\frac{4.8}{4}\right) = 2.6$$

The balanced reaction is now:



The air/fuel stoichiometric ratio is:

$$(A/F)_{stoic} = \frac{\text{no. of molecules of air}}{\text{no. of molecules of fuel}} \times \frac{\text{mol. wt. of air}}{\text{mol. wt. of fuel}}$$

$$(A/F)_{stoic} = \frac{4.76 \times 2.6 \times 28.85}{44.096}$$

$$(A/F)_{stoic} = 16.489$$